수의학박사 학위논문

Effects of cuprizone on hippocampal neurogenesis – Differential roles of melatonin and hypothermia

해마의 신경세포재생에 미치는 **cuprizone**의 영향에 대한 멜라토닌과 저체온증의 효과

2019 년 2 월

서울대학교 대학원

수의학과 수의해부학 전공

김 우 석

Effects of cuprizone on hippocampal neurogenesis – Differential roles of melatonin and hypothermia

Woosuk Kim

(Director: In Koo Hwang)

Department of Veterinary Medicine

Graduate School

Seoul National University

Abstract

Effects of cuprizone on hippocampal neurogenesis – Differential roles of melatonin and hypothermia

(Supervisor: In Koo Hwang, D.V.M., Ph.D)

Department of Veterinary Medicine

The Graduate School

Seoul National University

Cuprizone, a copper chelator, disrupts cell metabolism and causes demyelination and eventually neuronal degeneration such as oligodendritic and neuronal death. Cuprizone is widely used because of its convenience for experimental induction of neuronal degeneration by food and reversibility.

The aim of this study was to investigate the effects of cuprizone on adult hippocampal neurogenesis and cell damage in the naïve hippocampus in mice and ischemia-induced hippocampus in Mongolian gerbils. Additionally, we also observed the roles of melatonin and hypothermia on these effect. In the mouse experiment, 8-week-old male C57BL/6J mice were randomly divided into 3 groups: 1) control group and 2) groups treated with cuprizone only and 3) both cuprizone and melatonin. Cuprizone is administered by food at 0.2% ad libitum for 6 weeks. Melatonin is administered with tap water at 6 g/L ad libitum for 6 weeks;

the animals were then euthanized for immunohistochemistry of Ki67, doublecortin (DCX), glucose transporter 3 (GLUT3) and phosphorylation of cyclic AMP response element binding (pCREB), double immunofluorescence of neuronal nuclei (NeuN) and myelin basic protein (MBP), and western blot analysis of brain-derived neurotrophic factor (BDNF) expression to reveal the effects of cuprizone and melatonin on cell damage and hippocampal neurogenesis. In the gerbil forebrain ischemia experiment, 6-week-old male Mongolian gerbils were randomly divided into 6 group: 1) group that did not undergo ischemic brain surgery with normal diet, 2) group that did not undergo ischemic brain surgery with cuprizone diet, 3) group with that underwent normothermic ischemic brain surgery after 6 weeks of normal diet, 4) group that underwent normothermic ischemic brain surgery after 6 weeks of cuprizone diet, 5) group that underwent hypothermic ischemic brain surgery after 6 weeks of normal diet, and 6) group that underwent hypothermic ischemic brain surgery after 6 weeks of cuprizone diet. Cuprizone is also administered by food at 0.2% ad libitum. Forebrain ischemic surgery was performed with 5-min occlusion/reperfusion on the common carotid artery using aneurysm clips. Two weeks after ischemic surgery, all animals were sacrificed for cresyl violet (CV) staining and immunohistochemistry of DCX, Ki67, glial fibrillary acidic protein (GFAP), and ionized calcium-binding adapter molecule 1 (Iba-1) to reveal the effect of cuprizone on brain ischemia.

In the mouse experiment, administration of cuprizone significantly decreased the number of differentiating (DCX-positive) neuroblasts and proliferating (Ki67-positive) cells in the dentate gyrus (DG). Moreover, cuprizone administration decreased glucose utilization (GLUT3-positive cells) and cell transcription (pCREB-positive cells and BDNF protein expression) in the DG. Administration of

melatonin increased cuprizone-induced reduction in differentiating neuroblasts and proliferating cells, glucose utilization, and cell transcription. In the gerbil ischemia experiment, brain ischemia decreased cell survival (CV staining) and increased differentiating (DCX-positive) neuroblasts, proliferating (Ki67-positive) cells, reactive microglia (Iba-1-positive), and astrocytes (GFAP-positive). In contrast, hypothermic conditioning increased cell survival (CV staining) and decreased reactive microglia (Iba-1-positive) and astrocytes (GFAP-positive). However, cuprizone treatment decreased cell survival and increased reactive microglia and astrocytes. These change results from the fact that the protective effect of hypothermia in ischemic damage is disrupted due to cuprizone administration.

The results of the study suggest that cuprizone treatment disrupted hippocampal neurogenesis, which was enhanced by melatonin treatment. Additionally, cuprizone accelerated brain ischemic damage and disrupted the protective effect of hypothermia in brain ischemia.

Keywords: Cuprizone, Hippocampus, Neurogenesis, Forebrain ischemia, Hypothermia, Melatonin, C57BL/6 mouse, Mongolian gerbil,

Student Number : 2011-21683

Contents

Introduction

The hippocampus plays major roles in spatial memory as well as consolidation of long-term memory from short-term memory (Goodman et al., 2010) and consists of two arts: hippocampus proper and dentate gyrus (DG). The DG forms a V-shaped structure embedded in the curved cornus ammonis (CA), which is composed of the CA3, CA2, and CA1 regions of the hippocampus. Moreover, it can be subdivided into three layers: molecular layer (ML), polymorphic layer (PoL), and granule cell layer (GCL). The ML, the most superficial layer of the DG, consists of axons originating from the entorhinal cortex (EC) and also contains GABAergic interneurons. The GCL, the middle stratum of the DG, is formed by layers of cell bodies of granule cells, in which dendrites pass through the ML to receive the input signaling from the perforant pathway in the EC. The PoL, the deepest layer of the DG, contains not only axons from granule cells but also the mossy fiber, with most abundant interneuron. The subgranular zone (SGZ), the border between the GCL and hilum, is a region where adult neurogenesis occurs (Toni and Schinder, 2015).

Hippocampal neurogenesis has multiple steps wherein proliferative precursor cells become new granule cells in the DG. These multiple steps can be classified into four stages: 1) precursor cell phase, 2) arly survival phase, 3) postmitotic maturation phase, and 4) late survival phase (Kempermann et al., 2015). Hippocampal neurogenesis originates from precursor cells, and these cells are called “radial glia-like” cells because of their morphology (Kempermann et al., 2015). In the first stage, a precursor cell phase, the radial glial-like type 1 cells become type 2 cells that show higher proliferative activity. When type 1 cell becomes type 2 cells, it receives GABAergic synaptic input (Tozuka et al., 2005;

Wang et al., 2005). Physiological stimuli including voluntary wheel running (Kronenber et al., 2003) and serotonin-dependent mechanism (Encinas et al., 2006) activated type 2 cells, and gamma-aminobutyric acid (GABA) seems to be a regulator of these reactions (Ge et al., 2007). After the precursor cell phase, type 2 cell is neuronally determined and then becomes the type 3 cell, a proliferative late precursor cell. It exits from the cell cycle. It still has proliferative activity, but a dramatic elimination process occurs within a few days (Biebl et al., 2000; Kuhn et al., 2005). Therefore, the majority of cells that have no functional connection from the entorhinal cortex or CA1 are eliminated in this phase. In the third stage, the early postmitotic maturation phase, the cells become much more like neuronal cells. In this phase, the dendrites of the cell extend to the entorhinal cortex, the axon extends to CA1, and synaptic plasticity also increases (Kempermann et al., 2015). Only the cell that processes the synaptic input from the entorhinal cortex and output to CA1 an survive and proceed to the next stage (Kempermann et al., 2015). In the fourth stage, the late postmitotic maturation phase, dendritic spines mature, threshold for long term potential decreases, and synaptic plasticity increases (Kempermann et al., 2015). After this stage, the precursor cell becomes a hippocampal granule cell.

Cuprizone

Myelination means packing the conductor, “axon,” by a fatty material called “myelin” to increase the speed of transfer of information. Myelin is formed by “oligodendrocytes” in the central nervous system (CNS) and “Schwann cells” in the peripheral nervous system. The myelinated axon is much like an electric wire covered with insulating material. Demyelination is the opposite f myelination, so it

means that the insulating material, myelin, is peeled from the electric wire, axon. It may happen in pathological situations such as multiple sclerosis, which is a macerating neurological condition because of immune-mediated demyelination (Compston A and Coles, 2008).

Cuprizone, a copper chelator, disrupts cell metabolism and causes demyelination, and eventually oligodendritic and neuronal death (Gudi et al., 2014). Cuprizone is widely used because of its convenience for experimental induction of demyelination by food and reversibility. In the corpus callosum (CC), forming the roof of the subventricular zone (SVZ) of the DG, demyelination results from cuprizone treatment. Thus SVZ response to demyelination and remyelination in the CC can be investigated in cuprizone treatment (Hillis et al., 2016).

Copper, a cofactor of various cuproenzymes, plays crucial roles in many cellular processes, so coppr disturbance in the nervous system results in severe neuronal degeneration (Praet et al., 2014). Cuprizone acts as a copper chelator, so cuprizone administration causes copper deficiency and severe neuronal degeneration, such as demyelination of the CNS (Blakemore., 1972; Blakemor., 1973; Kesterson and Carlton., 1971; Ludwin, S., 1994; Pattison and Jebbett., 1971; Suzuki, K and Kikkawa, T., 1969). A decrease in the activity of cytochrome oxidase and other mitochondrial enzymes, such as monoamine oxidase in the brain resulted from administration of cuprizone (Venturini., 1973).

Melatonin as a neuroprotectant

Melatonin (N-acetyl-5-methoxytryptamine), a hormone produced by the pineal gland, is known to be associated with the day and night cycle, and it regulates wakefulness (Hardeland et al., 2006). The most common pathophysiological

mechanisms leading to neuronal death in neuronal degenerative diseases consist of three major interrelated processes. These are glutamate excitotoxicity, free radical-mediated damage and mitochondrial dysfunction (Reiter., 1998). Melatonin has been proposed as a neuroprotective agent against neuronal degenerative disease because of the following properties. Melatonin has direct and indirect antioxidant activity (Reiter et al., 2010). In studies on the effect of melatonin on antioxidative properties, melatonin has an antioxidative activity, scavenging free radicals more effectively than vitamins C and E (Calano et al., 2011). Moreover, melatonin has anti-excitotoxic actions; thus in previous studies, it was reported to prevent neuronal death induced by glutamate (Giusti et al., 1996; Manev et al., 1996) and hippocampal CA1 neuron injury (Cho et al., 1997; Kilic et al., 1999). In addition to these properties, melatonin has secondary antioxidative activity, regulating various enzymes relating to oxidative reaction such as upregulation of antioxidative enzymes and downregulation of pro-oxidative enzymes (Pandi-Perumal et al., 2013). Many therapeutic trials on melatonin suggested its potential therapeutic values as a neuroprotective drug in the treatment of various neurodegenerative diseases, such as Alzheimer's disease, Parkinson's disease, amyotrophic lateral sclerosis, and Huntington's disease (Pandi-Perumal et al., 2013).

Forebrain ischemia and hypothermia

Cerebral ischemia is a major cause of disability, acute mortality, chronic morbidity, and death worldwide (Soler and Ruiz., 2010). It results from reduction or loss of oxygen supply, and prolonged ischemia may lead to insidious delayed degeneration of specific vulnerable neurons within the affected brain region, including the hippocampus (Petito et al., 1997; Lin et al., 1990; Kirino., 1982). Oxidative stress

plays a key role in the pathophysiological cascade leading to brain-tissue injury. In particular, ischemia followed by reperfusion causes a rapid, transient increase in the production of reactive oxygen species (ROS) (Moskowitz et al., 2010). The resulting accumulation of free radicals in tissues can result in DNA damage and lipid peroxidation (Wang et al., 2013; Harput et al., 2012). Mitochondrial damage activates intracellular apoptotic signaling pathways and ultimately induces the activation of cysteine proteases of the caspase family (Gross et al., 1999; Green and Reed., 1998). Antioxidants have neuroprotective effects against ischemic damage because they neutralize ROS production and mitochondrial dysfunction (Hwang et al., 2010; Hwang et al., 2005; Eum et al., 2004).

The aim of this study was to investigate the effects of cuprizone on the adult hippocampal neurogenesis and cell damage in the naïve hippocampus in mice and ischemia-induced hippocampus in Mongolian gerbils. Additionally, we also observed the roles of melatonin and hypothermia on these effects.

Materials and methods

Experimental design 1

In experimental design 1, melatonin and cuprizone effects were investigated in C57BL/6 mice. Experimental animals were divided into 3 groups, and several markers were investigated with immunohistochemistry and western blot analysis (Fig. 1).

Experimental Animals

Eight-week-old male C57BL/6 mice were purchased from Jackson Laboratory Co. Ltd. (Bar Harbor, ME, USA). They were housed under standard conditions with feasible temperature (22 ± 2℃) and humidity (60 ± 5%) control and a 12:12 h light/dark cycle with ad libitum access to food and water. The handling and care of the animals conformed to guidelines of current international laws and policies (National Institutes of Health [NIH] Guide for the Care and Use of Laboratory Animals, Publication No. 85–23, 1985, revised 1996) and were approved by the Institutional Animal Care and Use Committee of Seoul National University. All experiments were conducted with an effort to minimize the number of animals used and the physiological stress caused by the procedures employed in the present study.

Experimental Groups and Treatment

The animals (n = 15) were divided into 3 groups as follows: 1) normal diet-fed (control) group, 2) cuprizone-containing diet-fed (cuprizone) group, and 3) melatonin-supplied cuprizone group (cuprizone + melatonin) group. Cuprizone diet was made by addition of 0.2% cuprizone to chow diets. Melatonin was dissolved in water (6 mg/L) and administered *ad libitum* for 6 weeks.

Tissue processing

The animals were anesthetized with 1 g/kg urethane (Sigma-Aldrich, St. Louis, MO, USA) 6 weeks after the first administration. Then, the thoracic cavity was opened and, perfused transcardially with 0.1 M phosphate buffered saline (PBS, pH 7.4) followed by 4% paraformaldehyde in 0.1 M phosphate buffer (PB, pH 7.4) using a flexible tube (HV-06409-16, Masterflex) with needle. The brains were then dissected and post-fixed for 12 h in the same fixative. The brain tissues were cryoprotected by overnight infiltration with 30% sucrose in 0.1 M PB. Serial brains were sectioned in the coronal plane at a thickness of 30 μm using a cryostat (Leica, Wetzlar, Germany) and collected in 6-well plates containing PBS for further processing.

Immunohistochemistry of DCX, Ki67, GLUT3 and pCREB

The sections were processed under the same conditions to obtain the comparable

immunohistochemistry among the groups. Three sections with 150-μm intervals between 1.82 and 2.32 mm posterior to the bregma, in reference to a mouse atlas (Paxinos and Franklin, 2001), were obtained from each animal. Each tissue section was sequentially treated with 0.3% H2O2 in PBS for 30 min and 10% normal goat serum in 0.1 M PBS for 30 min at 25℃. The sections were first incubated overnight with rabbit anti-doublecortin (DCX, 1:2000, Abcam), rabbit anti-glucose transporter 3 (GLUT3; 1:50, Santa Cruz Laboratory, Santa Cruz, CA), rabbit anti-Ki67 (1:1000; Abcam), or rabbit anti-phospho-cAMP response element-binding protein (pCREB, 1:400; Cell Signaling, Danvers, MA, USA) at 25℃. The next day, the sections were treated with biotinylated goat anti-rabbit IgG (1:200; Vector, Burlingame, CA) for 2 h at the room temperature (25℃). Then, the sections were treated streptavidin-peroxidase complex (1:200; Vector, Burlingame) for 2 h at 25ºC. Thereafter, the brain sections were visualized by reaction with 3,3'-diaminobenzidine tetrahydrochloride (DAB, Sigma) in 0.1 M Tris-HCl buffer (pH 7.2) and mounted on gelatin-coated slides. Sections were dehydrated with graded concentrations of alcohol and mounted in Canada balsam (Kanto Chemical, Tokyo, Japan).

Double immunofluorescence of neuronal nuclei and myelin basic protein

To confirm colocalization of neuronal nuclei (NeuN) and myelin basic protein (MBP) in the brain, the mouse sections were processed by double immunofluorescence staining. Tissue sections with 150-μm intervals between 1.82 and 2.32 mm posterior to the bregma, in reference to a mouse atlas (Paxinos and Franklin, 2001), were obtained from each animal. Each tissue section was

sequentially treated with 10% normal goat serum in 0.1 M PBS for 30 min at 25℃. The sections were first incubated overnight with the mixture antisera of mouse anti-NeuN (1:100; Merck Millipore) and rabbit anti-MBP (1:200; Merck Millipore) at 25℃. The next day, after washing in PBS 3 times, the sections were treated with a mixture of both Cy3-conjugated donkey anti-rabbit IgG (1:500; Jackson ImmunoResearch, PA, USA) and Alexa Fluor 488 AffiniPure donkey anti-mouse IgG (1:500; Jackson ImmunoResearch) with 4′,6-diamidino-2-phenylindole (1:1000, Sigma) for 2 h at 25 ○ C. Thereafter, the section was mounted on gelatin-coated slides and in a water soluble mounting medium, Fluoromount-G® (SouthernBiotech, AL, USA).

Western Blot Analysis

To confirm the effects of cuprizone and melatonin on hippocampal neurogenesis in mice, 6 animals in each group were sacrificed and used for western blot analysis. After removing the brain, the DG was dissected with a surgical blade. The tissues were homogenized in 50 mM PBS (pH 7.4) containing 0.1 mM ethylene glycol-bis(2-aminoethylether)-N,N,N′,N′-tetraacetic acid (pH 8.0), 0.2% Nonidet P-40, 10 mM ethylenediaminetetraacetic acid (pH 8.0), 15 mM sodium pyrophosphate, 100 mM β-glycerophosphate, 50 mM NaF, 150 mM NaCl, 2 mM sodium orthovanadate, 1 mM phenylmethylsulfonyl fluoride, and 1 mM dithiothreitol (DTT). After centrifugation, protein levels were determined in the supernatants using a Micro BCA protein assay kit with bovine serum albumin standards (Pierce Chemical, Rockford, IL). Samples containing 20-μg total protein were boiled in the loading buffer containing 150 mM Tris (pH 6.8), 3 mM DTT, 6% sodium dodecyl

sulfate, 0.3% bromophenol blue, and 30% glycerol. The samples were then loaded onto polyacrylamide gel. After electrophoresis, the proteins were transferred to nitrocellulose transfer membranes (Pall Corp, East Hills, NY). To reduce background staining, the membranes were incubated in 5% non-fat dry milk in PBS containing 0.1% Tween 20 for 45 min. The membrane was then incubated in rabbit anti-brain-derived neurotrophic factor (BDNF, 1:1000, Chemicon, Temecula, CA). After incubation in the primary antibodies, the membranes were incubated in peroxidase-conjugated anti-rabbit IgG, and the signal was developed with a luminol-based enhanced chemiluminescent kit (Pierce Chemical). The blot was scanned for the densitometric analysis of bands. Relative optical density (ROD) of each band was quantified using the Scion Image software (Scion Corp., Frederick, MD). Data were normalized for β-actin.

Statistical Analysis

Analysis of the regions of the hippocampal DG for GLUT3-positive cells and subcallosal zone (SCZ) for DCX- and pCREB-positive cells was performed using an image analysis system and ImageJ software (NIH Bethesda, MD, USA). To confirm objectivity, data were analyzed under the same conditions by two observers for each experiment in blinded conditions. Digital images of the whole DG and SCZ were captured with a BX51 light microscope (Olympus, Tokyo, Japan) equipped with a digital camera (DP72, Olympus) connected to a computer monitor. Images were calibrated into an array of 512 × 512 pixels corresponding to a tissue area of 1200 μm × 900 μm (100× primary magnification). Each pixel resolution had 256 gray levels, and the intensity of DCX, GLUT3, and pCREB

immunoreactivity was evaluated by ROD, which was obtained after transformation of the mean gray level using the following formula: ROD = log(256/mean gray level). The ROD of background staining was determined in unlabeled portions of the sections using Photoshop CC 2018 software (Adobe Systems Inc., San Jose, CA, USA), and this value was subtracted to correct for nonspecific staining using ImageJ software version 1.50. Data are expressed as percentage of the control group (set at 100%).

To compare immunohistochemistry for DCX, Ki67, and pCREB between the experimental groups, brain sections located 1.82 and 2.32 mm posterior to the bregma were selected for each animal. The number of DCX-, Ki67-, and pCREB-positive cells were counted using an analysis system with a computer-based CCD camera (OPTIMAS software version 6.5; CyberMetrics® Corporation, Phoenix, AZ, USA; magnification, 100×). All counts from all sections were averaged.

Results are shown as mean ± standard error of mean (SEM). Statistical analysis of data was performed using one-way analysis of variance (ANOVA), and further comparisons were assessed using Tukey's multiple-range test in order to elucidate the effects of cuprizone and melatonin on hippocampal neurogenesis in mice. A P-value < 0.05 was considered statistically significant.

Group(n=15)	1 week	2 week	3 week	4 week	5 week	6 week
Control (Normal Diet)						
Cuprizone [Cuprizone Diet(0.2%)]						
Cuprizone + Melatonin [Cuprizone Diet(0.2%) + Melatonin(6mg/L)]						

Figure. 1. Schematic workflow of experimental design 1.

Experimental design 2

In experimental design 2, hypothermia and cuprizone effects were investigated after transient forebrain ischemia in Mongolian gerbils. Experimental animals were divided into 6 groups: 1) group that did not undergo ischemic brain surgery with normal diet (Control group), 2) group that did not undergo ischemic brain surgery with cuprizone diet (Cuprizone group), 3) group that underwent normothermic ischemic brain surgery after 6 weeks of normal diet (Control+Isch group), 4) group that underwent normothermic ischemic brain surgery after 6 weeks of cuprizone diet (Cup+Isch group), 5) group that underwent hypothermic ischemic brain surgery after 6 weeks of normal diet (Control+Isch+HypoT group), and 6) group that underwent hypothermic ischemic brain surgery after 6 weeks of cuprizone diet (Cup+Isch+HypoT group). The animals in the groups were fed a normal diet or cuprizone-containing diet 6 weeks before ischemic surgery and 2 weeks after surgery. Every animal was sacrificed for tissue processing 2 weeks after ischemic surgery (Fig. 2).

Experimental Animals

Six-week-old male Mongolian gerbils were purchased from Japan SLC, Inc. (Shizuoka, Japan). Gerbils were housed in adequate temperature (22 ± 2℃) and humidity (60 ± 5%) with a 12-h light/12-h dark cycle with available access of food and tap water ad libitum. Handling and care of animals conformed to current international laws and policies (NIH Guide for the Care and Use of Laboratory Animals, NIH Publication No. 85-23, 1985, revised in 1996) and were approved by

the Institutional Animal Care and Use Committee of Kangwon National University.

Experimental groups and treatment

Gerbils (n = 5) were randomly divided into 6 groups as described above: Control, Cuprizone, Control+Isch, Cup+Isch, Control+Isch+HypoT, and Cup+Isch+HypoT groups. Cuprizone diet was made by addition of 0.2% cuprizone to chow diets. Normal diet and cuprizone-containing diet were administered ad libitum for 8 weeks to each animal in the groups.

Induction of transient forebrain ischemia

The animals were anesthetized with a mixture of 2.5% isoflurane (Baxter, Deerfield, IL, USA) in 33% oxygen and 67% nitrous oxide. Common carotid arteries were isolated and occluded bilaterally using non-traumatic aneurysm clips. Complete interruption of blood flow was confirmed by observing the central artery in the retinae using an ophthalmoscope (HEINE K180®; HEINE Optotechnik, Herrsching, Germany). The aneurysm clips were removed after 5 min of occlusion. Except the ischemia under the hypothermic condition groups, body temperature in each animal in the ischemic surgery groups was monitored under free-regulating or normothermic (37 ± 0.5℃) conditions with a rectal temperature probe (TR-100; Fine Science Tools, Foster City, CA, USA) and maintained using a thermometric blanket pre-, intra-, and postoperatively, until the animals completely recovered from anesthesia. In the ischemia under the hypothermic condition groups, body temperature was maintained under hypothermic (33.5 ± 0.5℃) condition with the

same methods described above. One animal was excluded due to incomplete occlusion of the common carotid arteries. The control groups underwent sham operation, which is the same surgical procedure without occlusion of common carotid arteries.

Tissue processing

The animals were anesthetized with 2 g/kg urethane (Sigma-Aldrich) 2 weeks after ischemia/reperfusion. Then, the thoracic cavity was opened and perfused transcardially with 0.1 M PBS (pH 7.4), followed by 4% paraformaldehyde in 0.1 M PB (pH 7.4) using a flexible tube (HV-06409-16, Masterflex) with a needle. Then, the brains were dissected and post-fixed for 12 h in the same fixative. The brain tissues were cryoprotected by overnight infiltration with 30% sucrose in 0.1 M PB. Serial brains were sectioned in the coronal plane at a thickness of 30 μm using a cryostat (Leica, Wetzlar, Germany) and collected in 6-well plates containing PBS for further processing. The sections were processed under the same conditions to ensure that the immunohistochemical data were comparable among the groups. Tissue sections between 1.4 and 2.0 mm posterior to the bregma, in reference to a gerbil atlas (Loskota et al., 1974), were selected for each animal.

CV staining quantification

The sections were stained with cresyl violet (CV) acetate with the method described below. The sections were mounted on gelatin-coated microscope slides. CV acetate (Sigma) was dissolved in distilled water at 1% with glacial acetate at

0.25%. The brain sections were washed in distilled water 5 min before and after staining. Subsequently, the brain sections were dehydrated with continuous concentration of alcohol and cleared with xylene in 10 min for 3 times and mounted using Canada balsam (Kanto Chemical, Tokyo, Japan).

Immunohistochemistry DCX, Ki67, GFAP and Iba-I

Four sections, with 150-μm intervals between 1.4 and 2.0 mm posterior to the bregma, were sequentially treated with 0.3% H2O2 in PBS for 30 min and 10% normal goat serum in 0.05 M PBS for 30 min at 25℃. Sections were incubated with rabbit anti-DCX (1:2000, Abcam), rabbit anti-Ki67 antibody (1:1000; Abcam), rabbit anti-glial fibrillary acidic protein (GFAP; 1:1000, Chemicon International, Billerica, MA), or rabbit anti-ionized calcium-binding adapter molecule 1 (Iba-1; 1:500; Wako, Osaka, Japan) at 25℃ overnight. Thereafter, the sections were treated with biotinylated goat anti-rabbit IgG (1:200; Vector) for 2 h at 25℃. Then, the sections were treated with streptavidin-peroxidase complex (1:200; Vector) for 2 h at 25℃. Sections were visualized by reaction with DAB (Sigma) in 0.1 M Tris-HCl buffer (pH 7.2) and mounted on gelatin-coated slides. Sections were dehydrated and mounted in Canada balsam (Kanto Chemical, Tokyo, Japan). The sections were treated with anti-DCX antibody or fluorescein-AffiniPure donkey anti-rabbit IgG (1:200; Jackson ImmunoResearch, West Grove, PA, USA) with 4′ ,6-diamidino-2-phenylindole (1:1000, Sigma). Thereafter, the section was mounted on gelatin-coated slides and in water-soluble mounting medium, Fluoromount-G® (SouthernBiotech).

Semi-quantification of Data

CV-positive neurons, Ki67-positive proliferating cells, and pCREB-positive cells were identified in all groups using an image analysis system equipped with a computer-based charge-coupled device camera (software: Optimas® 6.5, CyberMetrics, Scottsdale, AZ). The number of CV-positive neurons was counted in the stratum pyramidale (SP) of the CA1 region, and the number of Ki67- and pCREB-positive proliferating cells was counted in the DG. Images of all CV-positive structures in the hippocampal CA1 region and Ki67-positive cells in the DG were captured using a BX51 light microscope (Olympus, Tokyo, Japan) equipped with a digital camera (DP71, Olympus). Cell counts were obtained by averaging the counts from the sections taken from each animal, and the numbers were presented as percentage of control or numbers per section.

Analysis of the regions of interest in the hippocampal DG region of DCX-positive neuroblasts was performed using an image analysis system. Images were calibrated into an array of 512 × 512 pixels corresponding to a tissue area of 140 μm × 140 μm (40× primary magnification). Pixel resolution was 256 gray levels. The intensity of DCX immunoreactivity was evaluated by ROD, which was obtained after transformation of the mean gray level using the formula: ROD = log(256/mean gray level). The ROD of the background was determined in unlabeled portions (white matter region), and this value was subtracted to normalize the corrected optical densities using ImageJ 1.50 software (NIH, Bethesda). The ratio of the ROD was calculated as percentage relative to the control group.

Statistical Analysis

The results are shown as mean ± SEM. Statistical analysis of data was performed using one-way ANOVA, and further comparisons were assessed using Tukey's multiple-range test in order to elucidate the effects of cuprizone and hypothermia on hippocampal neurogenesis on the global forebrain ischemia model of gerbils. A P-value < 0.05 was considered statistically significant.

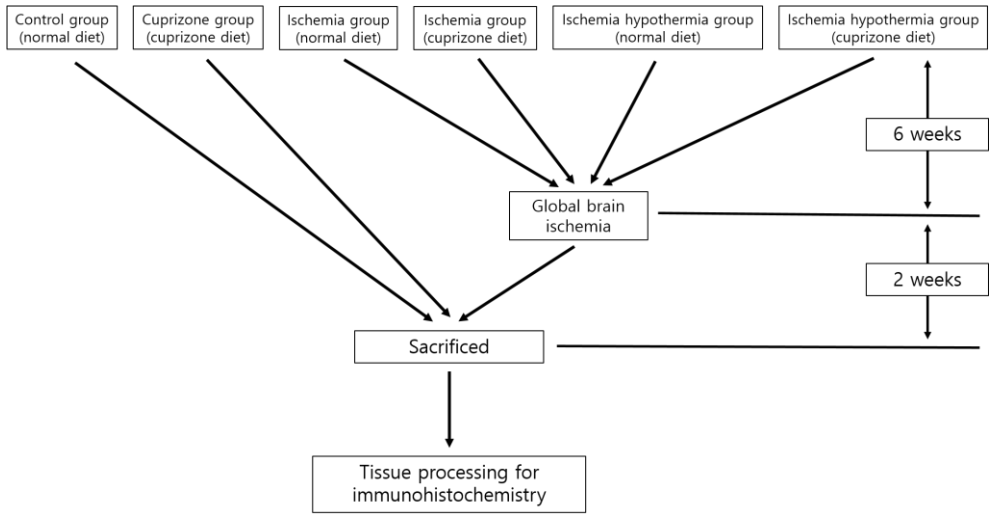

Figure. 2. Schematic workflow of experimental design 2.

Results

Experimental design 1

Neuroblast differentiation in the DG and SCZ

In the control group, DCX-positive neuroblasts were observed in the SGZ of the DG (Fig. 3A). In the cuprizone group, immunoreactivity of DCX-positive neuroblasts was significantly decreased in the DG compared to that of the control group (Fig. 3C). In the cuprizone + melatonin group, immunoreactivity of DCX-positive cells in the DG was significantly increased compared to that in the cuprizone group (Fig. 3E). The mean percentages of ROD were 23.9% in the cuprizone group and 52.3% in the cuprizone + melatonin group compared with 100% in the control group (Fig. 3G).

In contrast, few DCX-positive neuroblasts were observed in the SCZ of the control group (Fig. 3B). In the cuprizone group, immunoreactivity of DCX-positive neuroblasts was increased compared to that in the control group, but statistical significance was not found between the control and cuprizone groups (Fig. 3D). In the cuprizone + melatonin group, immunoreactivity of DCX-positive neuroblasts was significantly increased in the DG compared to that in the cuprizone group (Fig. 3F). The mean percentages of ROD were 120.6% in the cuprizone group and 204.8% in the cuprizone + melatonin group compared with 100% in the control group (Fig. 3H).

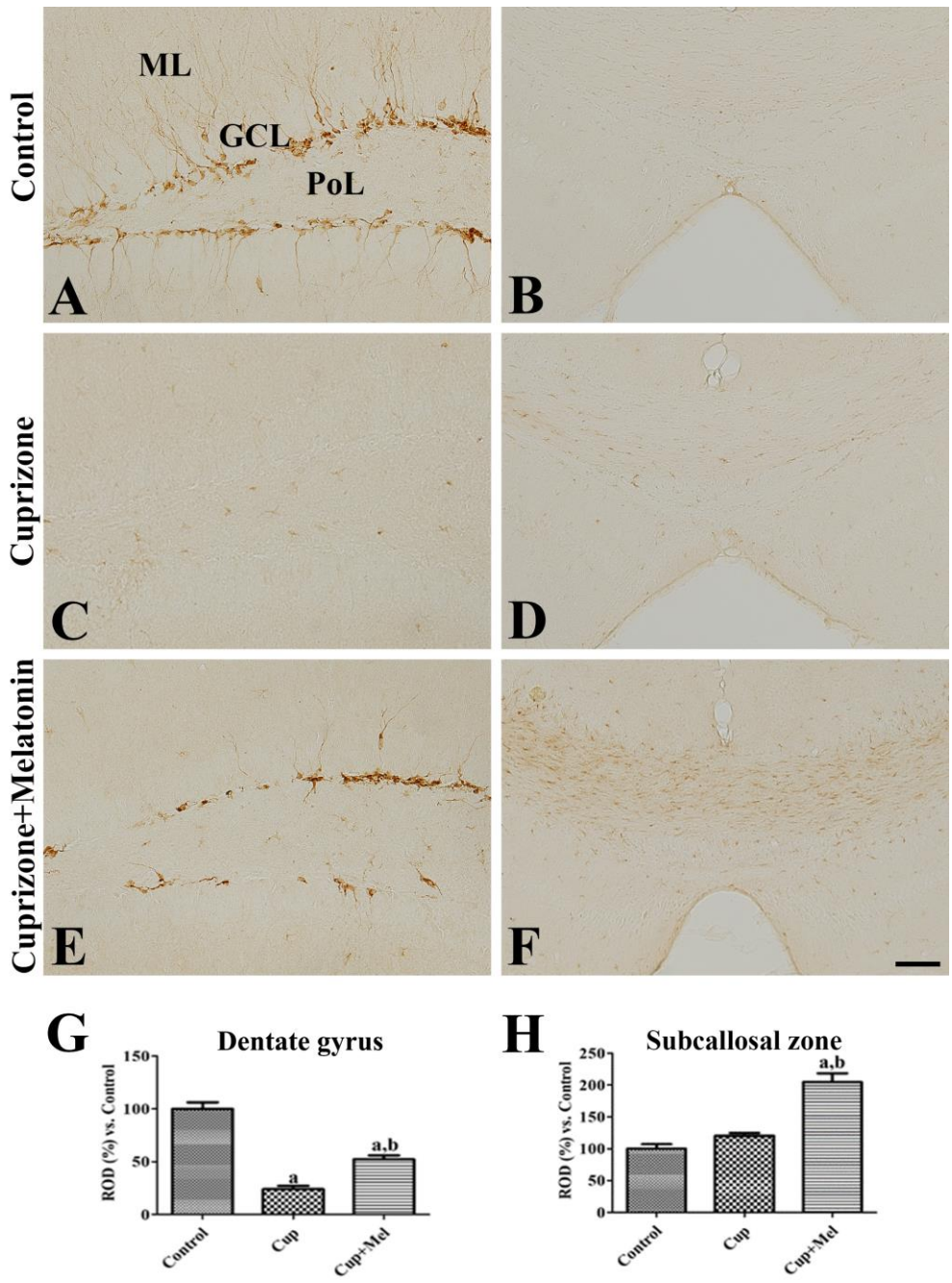
Control
Cuprizone
Cuprizone+Melatonin
ML
GCL
PoL
A
B
C
D
E
F
G
Dentate gyrus
ROD (%) vs. Control
150
100
50
0
a
a,b
Control
Cup
Cup+Mel
H
Subcallosal zone
ROD (%) vs. Control
250
200
150
100
50
0
a,b
Control
Cup
Cup+Mel

Figure 3. Immunohistochemistry for DCX in the DG and SCZ of the control (A and B), cuprizone (C and D), and melatonin + cuprizone groups (E and F). GCL, granule cell layer; ML, molecular layer; PoL, polymorphic layer. Scale bar = 50 μm (n = 9 per group, $^{a}P < 0.05$, significantly different from the control group; $^{b}P < 0.05$, significantly different from the cuprizone group). The bars indicate the standard error of the mean (SEM).

Cell proliferation in DG

In the control group, Ki67-positive cells were mainly observed in the SGZ of the DG (Fig. 4A). The number of Ki-67-positive cells per section was 9.5 in this group (Fig. 4D). In the cuprizone group, the number of Ki67-positive cells, which was 3.8, was significantly decreased compared to those in the control group (Fig. 4B and 4D). In the cuprizone + melatonin group, the number of Ki67-positive cells, which was 6.2, was increased compared to those in the cuprizone groups (Fig. 4C and 4D).

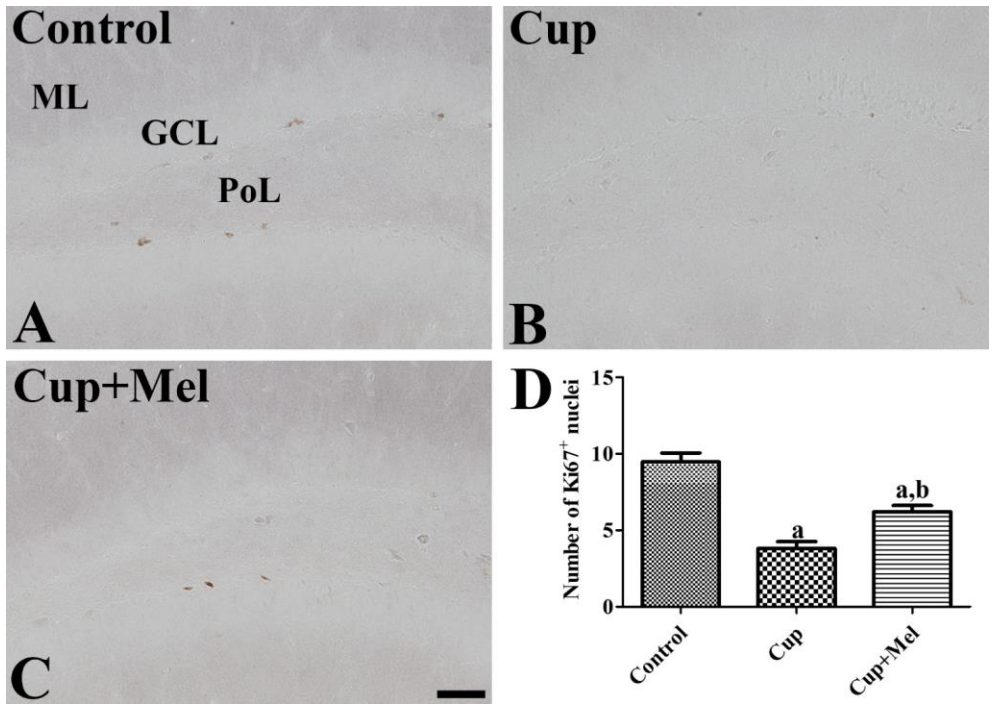

Figure 4. Immunohistochemistry for Ki67 in the DG of the control (A), cuprizone group (B), and cuprizone + melatonin groups (C). GCL, granule cell layer; ML, molecular layer; PL, polymorphic layer. Scale bar = 50 μm (D). Number of Ki67-positive cells per section in all groups (n = 9 per group; $^{a}P < 0.05$, significantly different from the control group; $^{b}P < 0.05$, significantly different from the cuprizone group). The bars indicate the standard error of mean (SEM).

Expression of GLUT3 in the hippocampal DG

Immunohistochemistry for GLUT3 was performed to evaluate glucose utilization in the hippocampal DG after cuprizone and melatonin treatment. GLUT3-immunopositive cells were mainly detected in the SGZ of the DG in the control group (Fig. 5A). In the cuprizone group, GLUT3 immunoreactivity was significantly decreased in the DG compared with that in the control group (Fig. 5B). In the cuprizone + melatonin group, GLUT3 immunoreactivity was significantly increased compared to that in the cuprizone group (Fig. 5C). The mean percentages of ROD were 34.3% in the cuprizone group and 78.2% in the cuprizone + melatonin group compared with 100% in the control group (Fig. 5D).

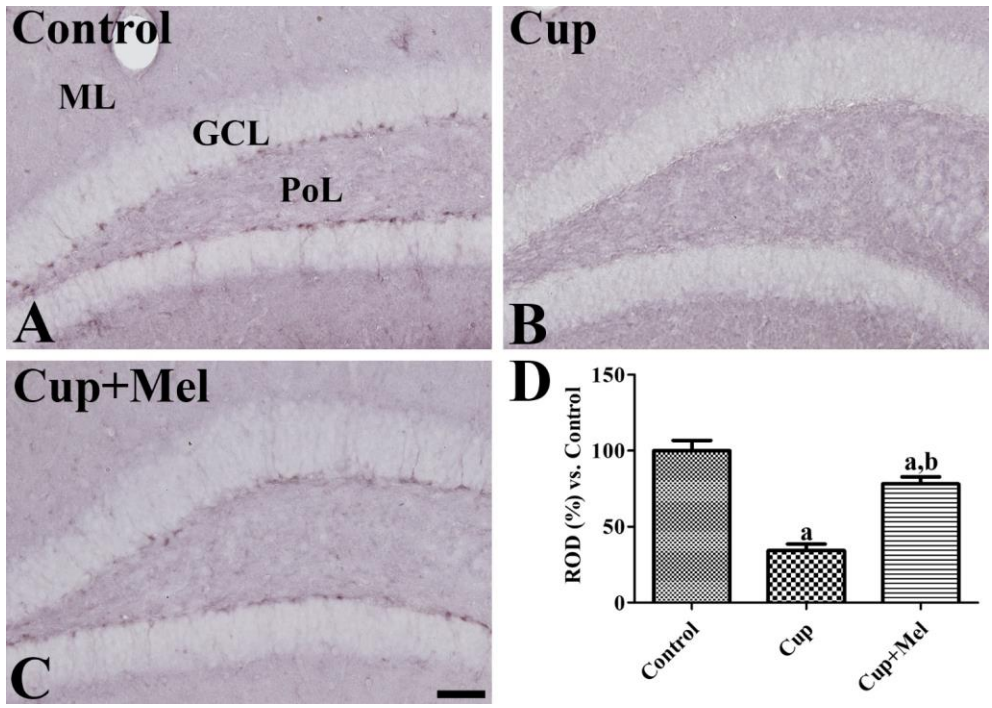

Figure 5. Immunohistochemistry for glucose transporter 3 (GLUT3) in the DG of the control (A), cuprizone (B), and cuprizone + melatonin groups (C). GCL, granule cell layer; ML, molecular layer; PoL, polymorphic layer. Scale bar = 50 μm (n = 9 per group, $^{a}P < 0.05$, significantly different from the control group; $^{b}P < 0.05$, significantly different from the cuprizone group). The bars indicate the standard error of mean (SEM).

Phosphorylation of CREB in the DG and SCZ

In the control groups, pCREB-positive nuclei were mainly found in the SGZ of DG (Fig. 6A). In the cuprizone group, the number of pCREB-positive nuclei was significantly decreased in the DG compared to that in the control group (Fig. 6C). In the cuprizone + melatonin group, pCREB-positive nuclei were significantly increased in the SGZ of DG compared with those in the control and cuprizone groups (Fig. 6E). The numbers of pCREB-positive nuclei were 53.1, 28.1, and 71.0 in the control, cuprizone, and cuprizone + melatonin groups, respectively (Fig. 6G). In the SCZ, decreased pCREB immunoreactivity was observed in the control group (Fig. 6B). In the cuprizone and cuprizone + melatonin groups, pCREB immunoreactivity significantly increased compared with that of the control group, especially the cuprizone + melatonin group (Fig. 6D and 6F). The mean RODs were 1060.5% in the cuprizone group and 1521.1% in the cuprizone + melatonin group compared with 100% in the control group (Fig. 6H).

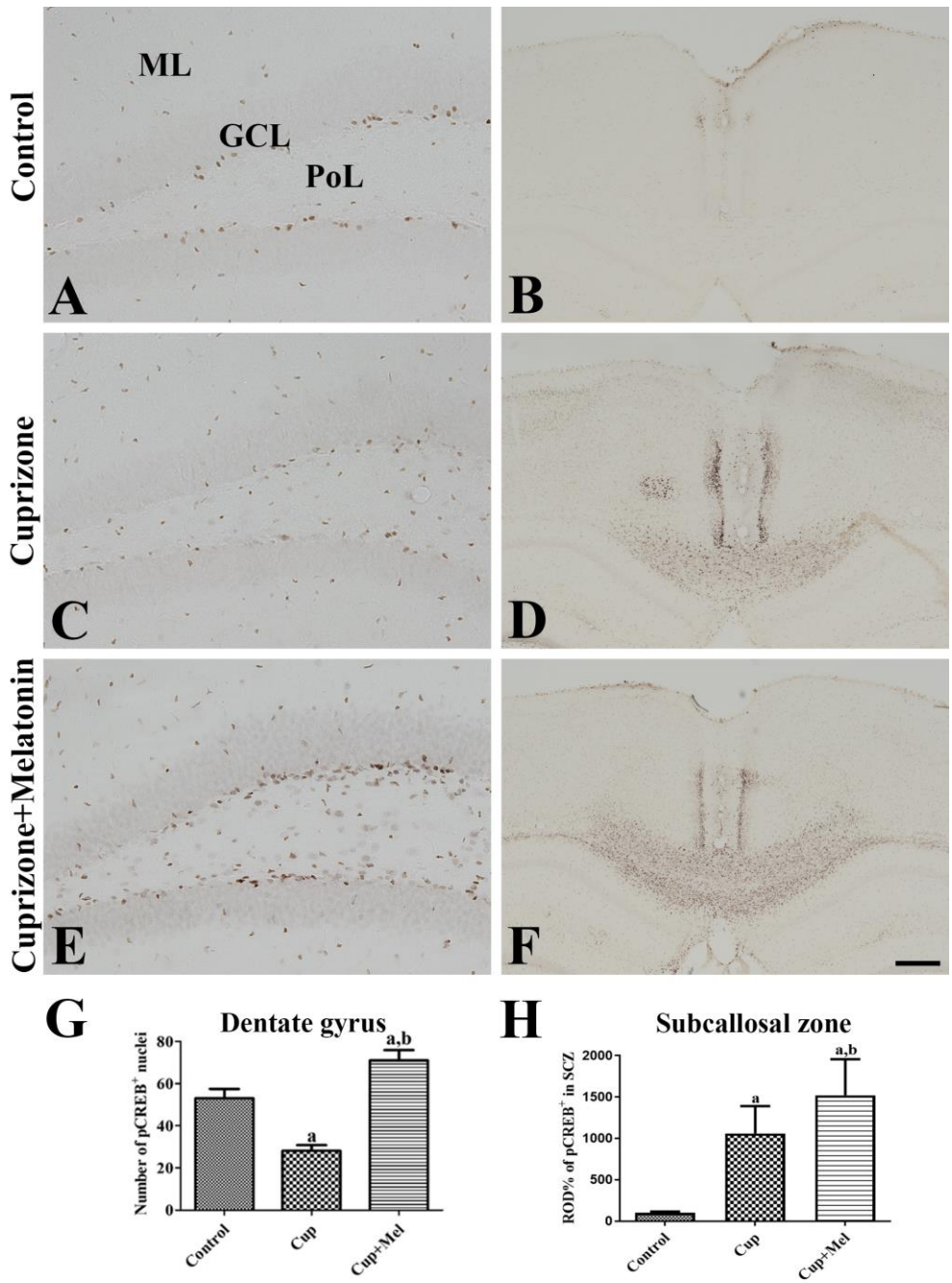
Control
Cuprizone
Cuprizone+Melatonin
ML
GCL
PoL
A
B
C
D
E
F
G
Dentate gyrus
Number of pCREB+ nuclei
a
a,b
Control
Cup
Cup+Mel
H
Subcallosal zone
ROD% of pCREB+ in SCZ
a
a,b
Control
Cup
Cup+Mel

Figure 6. Immunohistochemistry for pCREB in the DG (A, C, and E) and SCZ (B, D, and F) in the control (A and B), cuprizone (C and D), and cuprizone + melatonin groups (E and F). GCL, granule cell layer; ML, molecular layer; PoL, polymorphic layer. Scale bar = 50 μm (n = 9 per group, $^{a}P < 0.05$, significantly different from the control group; $^{b}P < 0.05$, significantly different from the cuprizone group). The bars indicate the standard error of mean (SEM).

Expression of NeuN and MBP in the hippocampus

There were no differences in NeuN- and DAPI-positive nuclei in the hippocampus among the control, cuprizone, and cuprizone + melatonin groups (Fig. 7A, 7C, 7E, 7G, 7I, and 7K). However, MBP immunoreactivity in the cuprizone group was decreased in the PoL, alveus, and stratum lacunosum moleculare (SLM) of the hippocampus compared to those in the control group (Fig. 7F). In the cuprizone + melatonin group, MBP immunoreactivity increased in the hippocampus compared to that in the cuprizone group (Fig. 7J), especially in the alveus and SLM.

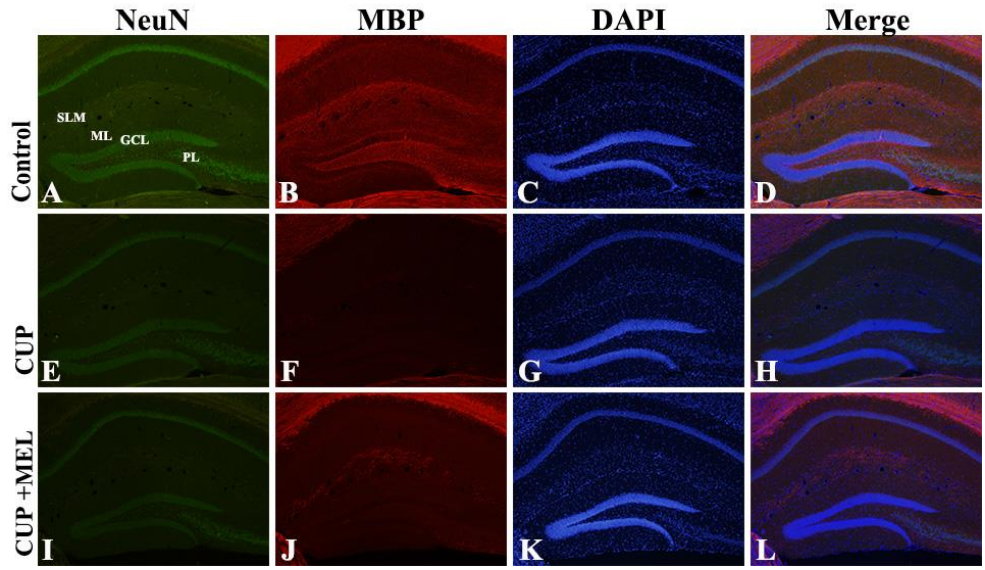

Figure 7. Double immunofluorescence staining for NeuN (A, E, and I, green), MBP (B, F, and J, red), DAPI (C, G, and K, blue), and merged image (D, H, L) in the hippocampus of mice in the control, cuprizone, and cuprizone + melatonin groups. GCL, granule cell layer; ML, molecular layer; PoL, polymorphic layer; SLM, stratum lacunosum moleculare (n = 9 per group).

BDNF protein expression in the hippocampus

Western blot analysis for BDNF was performed in all animal groups to confirm cuprizone and melatonin treatment effect on BDNF expression in the hippocampus (Fig. 8). In the cuprizone group, BDNF expression significantly decreased compared to that in the control group. The mean percentage of ROD was 41.8% compared with 100% in the control group (Fig. 8). In the cuprizone + melatonin group, the expression of level of BDNF significantly increased compared to that in the cuprizone group. The mean percentage of ROD was 72.5% compared with 100% in the control group (Fig. 8).

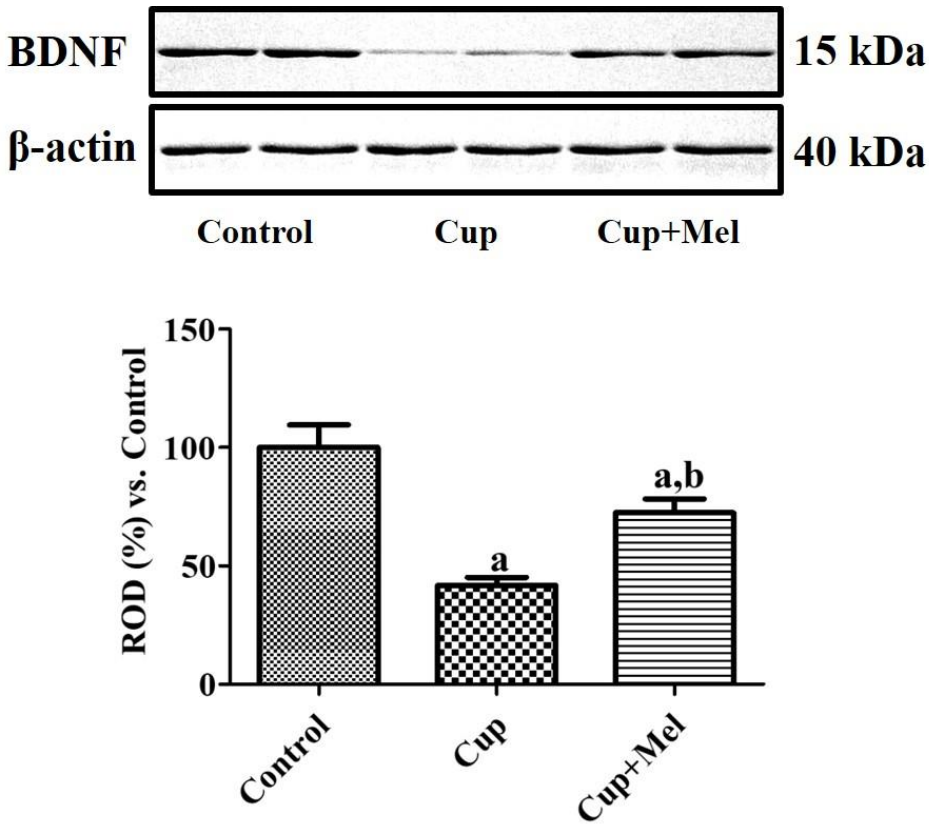

Figure 8. Western blot analysis of brain-derived neurotrophic factor (BDNF) in the hippocampi of mice in the control, cuprizone, and cuprizone + melatonin groups. ROD in the cuprizone and cuprizone + melatonin groups versus that in the control group is shown in percentages (n = 6 per group, $^{a}P < 0.05$, significantly different from the control group; $^{b}P < 0.05$, significantly different from the cuprizone group).

Experimental design 2

CV staining

To observe survived neurons in the hippocampal CA1 region after ischemic surgery, CV staining was performed in all experimental groups (Fig. 9). In the Control group, CV-positive neurons were abundant in SP (Fig. 9A and 9B). In the Control+Isch group, very few CV-positive neurons were detected in SP (Fig. 9C and 9D). In the Cup+Isch group, similar CV-positive neurons were observed in the CA1 region compared to that in the Control+Isch group (Fig. 9E and 9F). The number of CV-positive cells per section in the Control+Isch and Cup+Isch groups was 5.1% and 4.9%, respectively, of that in the Control group (Fig. 9K).

In the Control+Isch+HypoT group, CV-positive neurons in SP were increased compared to that in the Control+Isch group (Fig. 9G and 9H). In this group, the number of CV-positive neurons was 53.4% of that in the Control group (Fig. 9K). In Cup+Isch+HypoT group, CV-positive neurons in SP were decreased compared to that in the Control+Isch+HypoT group (Fig. 9I and 9J), but the number of CV-positive neurons were abundant compared to that in the Control+Isch group (Fig. 9K).

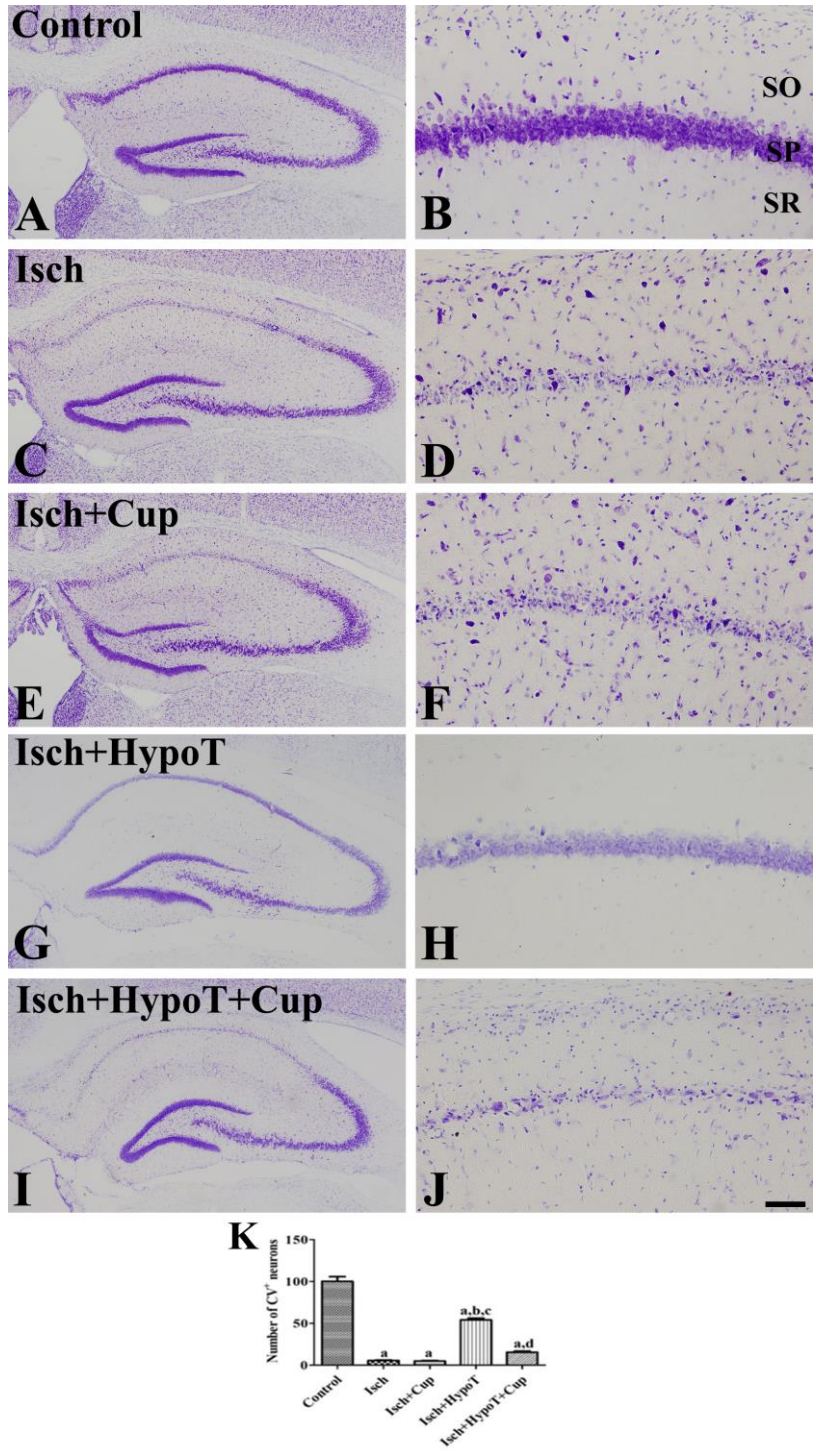
Control
A
B
SO
SP
SR
Isch
C
D
Isch+Cup
E
F
Isch+HypoT
G
H
Isch+HypoT+Cup
I
J
K
Number of CV+ neurons
150
100
50
0
a
a
a,b,c
a,d
Control
Isch
Isch+Cup
Isch+HypoT
Isch+HypoT+Cup

Figure 9. CV staining in the hippocampus of the Control (A and B), Control+Isch (C and D), Cup+Isch (E and F), Control+Isch+HypoT (G and H), and Cup+Isch+HypoT groups (I and J). SP, stratum pyramidale; SO, stratum oriens; SR, stratum radiatum. Scale bar = 50 μm (n = 5 per group, $^{a}P < 0.05$, significantly different from the Control group; $^{b}P < 0.05$, significantly different from the Control+Isch group; $^{c}P < 0.05$, significantly different from the Cup+Isch group; $^{d}P < 0.05$, significantly different from the Control+Isch+HypoT group). The bars indicate the standard error of mean (SEM).

Neuroblast differentiation in DG

In the Control group, DCX-positive neuroblasts were detected in the DG (Fig. 10A). In the Cup group, a few DCX-immunoreactive neuroblasts were found in the SGZ of the DG (Fig. 10B), and DCX immunoreactivity dramatically decreased by 35.4% of that in Control group (Fig. 10G). In the Control+Isch group, DCX-immunoreactive neuroblasts were abundantly found in the DG, and mean percentages of ROD in this group was 193.1% of that in the Control group (Fig. 10C and 10G). In the Cup+Isch group, DCX immunoreactivity was similarly observed in the Control group (Fig. 10D). In the Control+Isch+HypoT group, DCX-immunoreactive neuroblasts were most abundantly observed in the DG (Fig. 10E), while, in the Cup+Isch+HypoT group, DCX-immunoreactive neuroblasts were less abundantly observed (Fig. 10F). The mean percentages of ROD in the Control+Isch+HypoT and Cup+Isch+HypoT groups were 240.4% and 168.4%, respectively, compared with 100% in the control group (Fig. 10G).

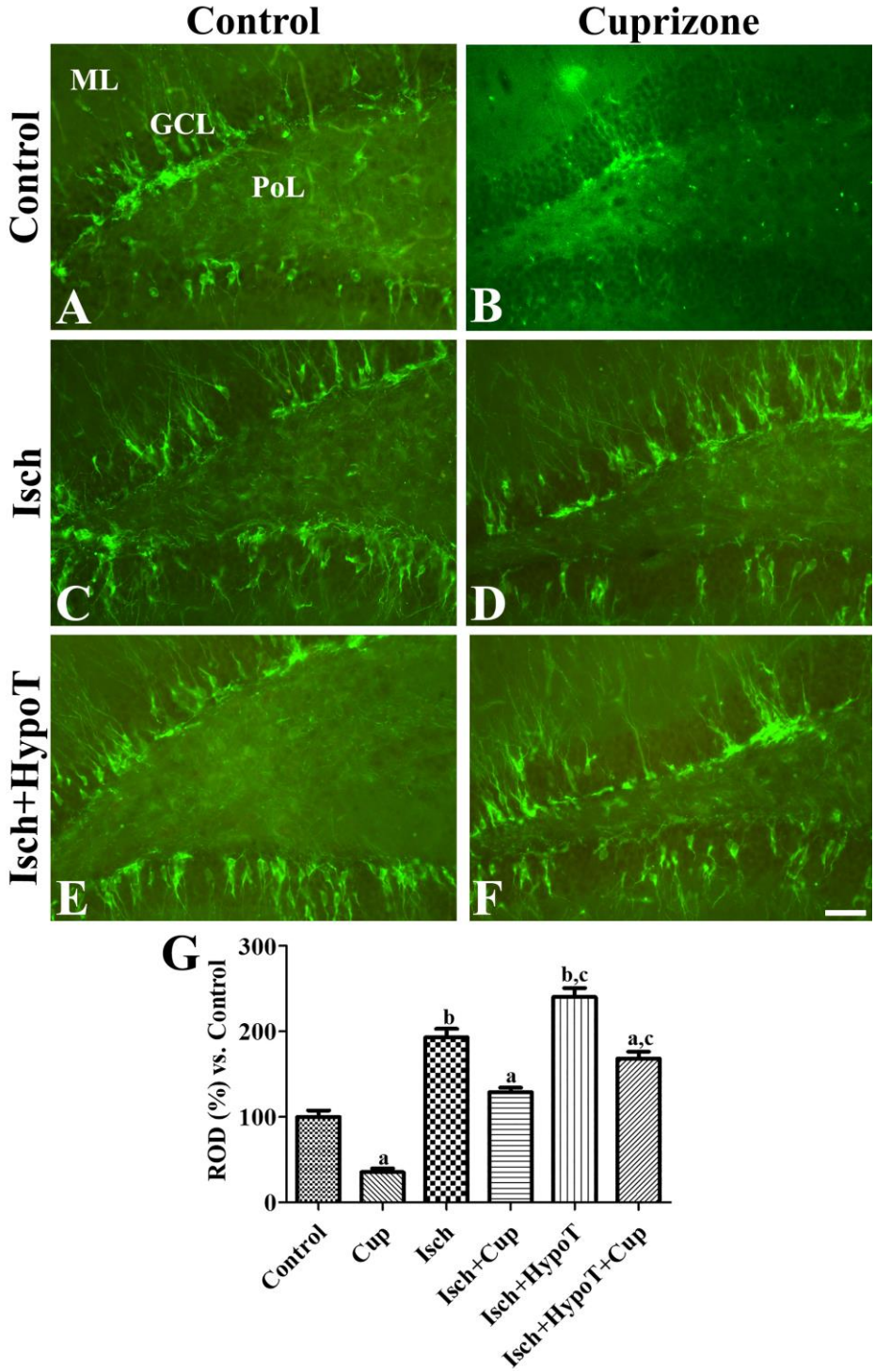
Control
Cuprizone
Control
Isch
Isch+HypoT
ML
GCL
PoL
A
B
C
D
E
F
G
ROD (%) vs. Control
300
200
100
0
a
b
a
b,c
a,c
Control
Cup
Isch
Isch+Cup
Isch+HypoT
Isch+HypoT+Cup

Figure 10. DCX immunohistochemistry in the gerbil hippocampal DG region of the Control (A), Cup (B), Control+Isch (C), Cup+Isch (D), Control+Isch+HypoT (E), and Cup+Isch+HypoT groups (F). GCL, granule cell layer; ML, molecular layer; PoL, polymorphic layer. Scale bar = 50 μm (n = 5 per group, $^{a}P < 0.05$, significantly different from the normal diet groups; $^{b}P < 0.05$, significantly different from the Control group; $^{c}P < 0.05$, significantly different from ischemia under normothermic condition with the normal or cuprizone-containing diet group). The bars indicate the standard error of mean (SEM).

Cell proliferation in DG

In the Control group, Ki67-positive cells were detected in the DG (Fig. 11A). The number of Ki67-positive cells per section was 17.3 (Fig. 11G). In the Cup group, Ki67-positive cells decreased in the DG (Fig. 11B), and the number of Ki67-positive cells per section was 11.9 (Fig. 11G). In the Control+Isch group, Ki67-positive cells increased compared to that of the control group, and the number per section was 44.0 (Fig. 11C and 11G). In the Cup+Isch group, Ki67-positive cells were similarly detected in the DG compared to that in the Cup group (Fig. 11D). In the Control+Isch+HypoT group, Ki67-positive cells decreased compared to that in Control+Isch group, and the number per section was 32.6 (Fig. 11E and 11G). In the Cup+Isch+HypoT group, a few Ki67-positive cells were found in the DG (Fig. 11F), and the number of Ki67-positive cells per section was 12.1 (Fig. 11G).

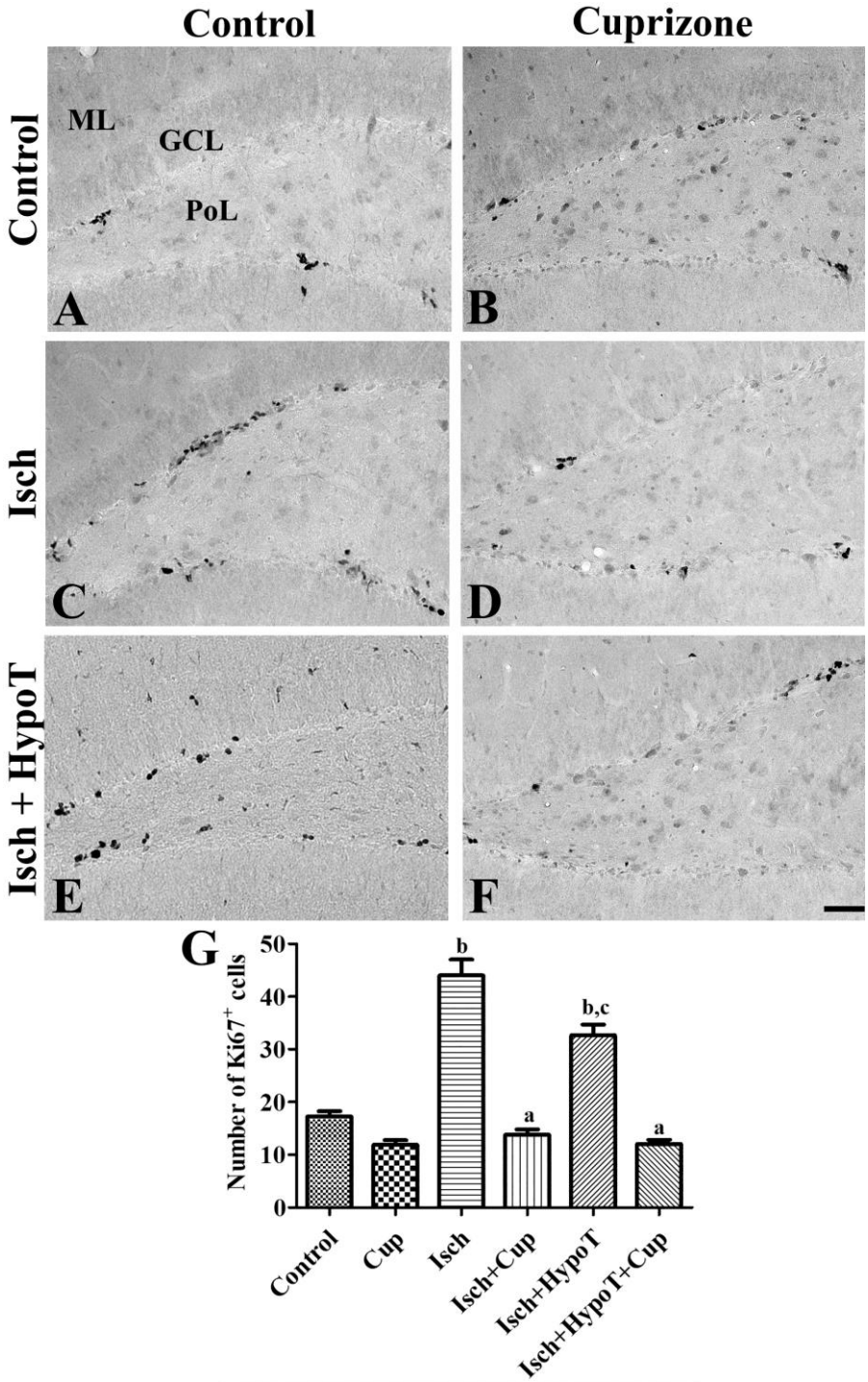
Control
Cuprizone
Control
Isch
Isch + HypoT
ML
GCL
PoL
A
B
C
D
E
F
G
Number of Ki67+ cells
50
40
30
20
10
0
b
a
b,c
a
Control
Cup
Isch
Isch+Cup
Isch+HypoT
Isch+HypoT+Cup

Figure 11. Ki67 immunohistochemistry in the gerbil hippocampal DG region of the Control (A), Cup (B), Control+Isch (C), Cup+Isch (D), Control+Isch+HypoT (E), and Cup+Isch+HypoT groups (F). GCL, granule cell layer; ML, molecular layer; PoL, polymorphic layer. Scale bar = 50 μm (n = 5 per group, $^{a}P < 0.05$, significantly different from the normal diet groups; $^{b}P < 0.05$, significantly different from the Control group; $^{c}P < 0.05$, significantly different from the Control+Isch group). The bars indicate the standard error of mean (SEM).

Expression of reactive astrocyte in the hippocampal CA1 region

In the Control group, GFAP-positive astrocytes had small cytoplasm with long thread-like process (resting form of astrocytes) in the hippocampal CA1 region (Fig. 12A). In the Cup group, a similar expression pattern of GFAP-positive astrocytes was observed in the hippocampal CA1 region compared to that in the Control group (Fig. 12B). In the Control+Isch group, GFAP-positive astrocytes had hypertrophied cytoplasm with thick process (reactive form of astrocytes) (Fig. 12C). In the Cup+Isch group, GFAP-positive astrocytes showed similar morphology in the hippocampal CA1 region in the Control+Isch group, and some of them had punctuated cytoplasm (Fig. 12D). In the Control+Isch+HypoT group, only a few GFAP-positive astrocytes had hypertrophied cytoplasm, but many of them showed resting forms of astrocytes (Fig. 12E). In the Cup+Isch+HypoT group, many GFAP-positive astrocytes were in activated form in the hippocampal CA1 region (Fig. 12F).

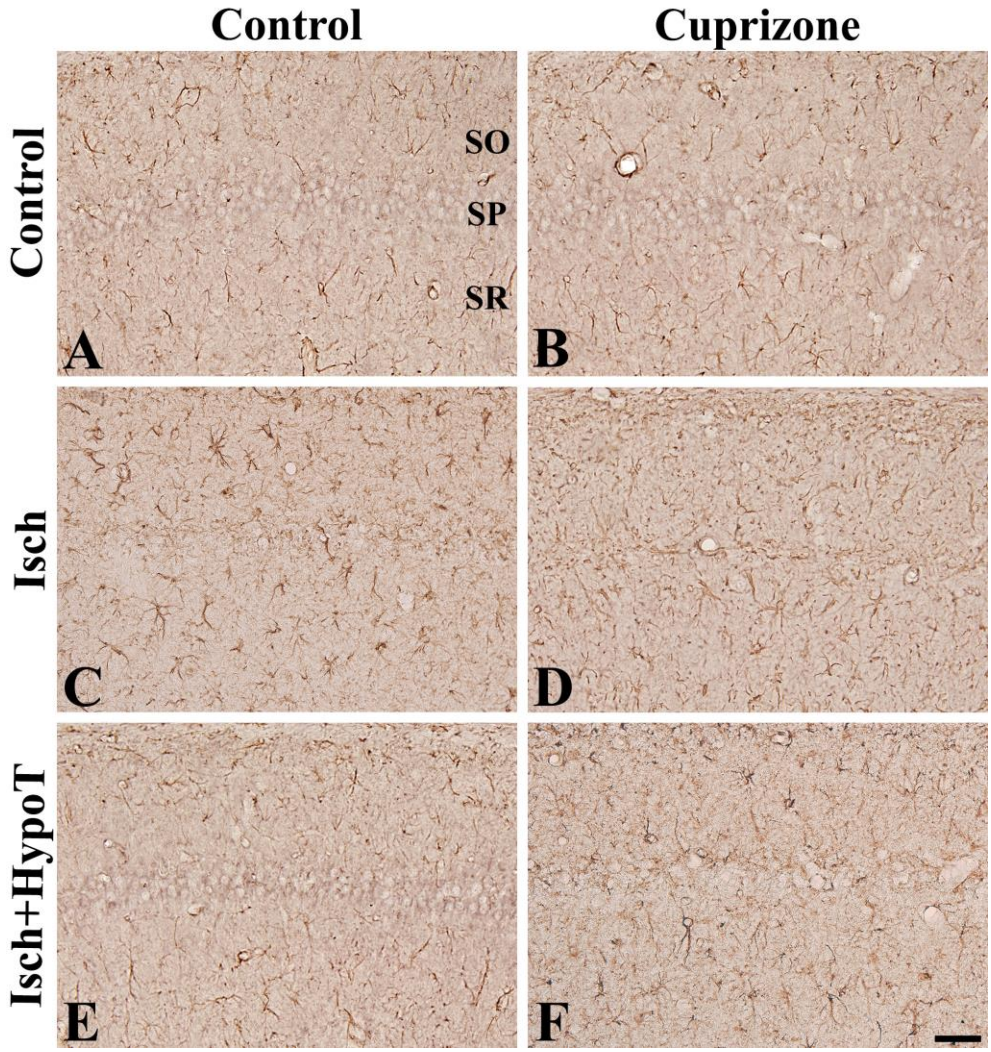
Control
Cuprizone
Control
Isch
Isch+HypoT
SO
SP
SR
A
B
C
D
E
F

Figure 12. GFAP immunohistochemistry in the gerbil hippocampal CA1 region of the Control (A), Cup (B), Control+Isch (C), Cup+Isch (D), Control+Isch+HypoT (E), and Cup+Isch+HypoT groups (F). SP, stratum pyramidale; SO, stratum oriens; SR, stratum radiatum. Scale bar = 50 μm (n = 5 per group)

Expression of reactive microglia in CA1

Iba-1-positive microglia were detected in the CA1 region of the hippocampus. In the Control group, Iba-1-positive microglia had small cytoplasm with thin processes (Fig. 13A). In the Cup group, Iba-1-positive microglia also had small cytoplasm with ramified processes (Fig. 13B). In the Control+Isch group, Iba-1-positive microglia had hypertrophied cytoplasm with thickened processes. In addition, round type of Iba-1-positive microglia was also found in the SP (Fig. 13C). In the Cup+Isch group, the distribution pattern and morphology of Iba-1-positive microglia was similar to that in the Control+Isch group (Fig. 13D). In the Control+Isch+HypoT group, some Iba-1-positive microglia had hypertrophied cytoplasm, but others had small cytoplasm (Fig. 13E). In the Cup+Isch+HypoT group, many Iba-1-positive microglia with hypertrophied cytoplasm were found in the SR, while round-type Iba-1-positive microglia were observed in the SP (Fig. 13F).

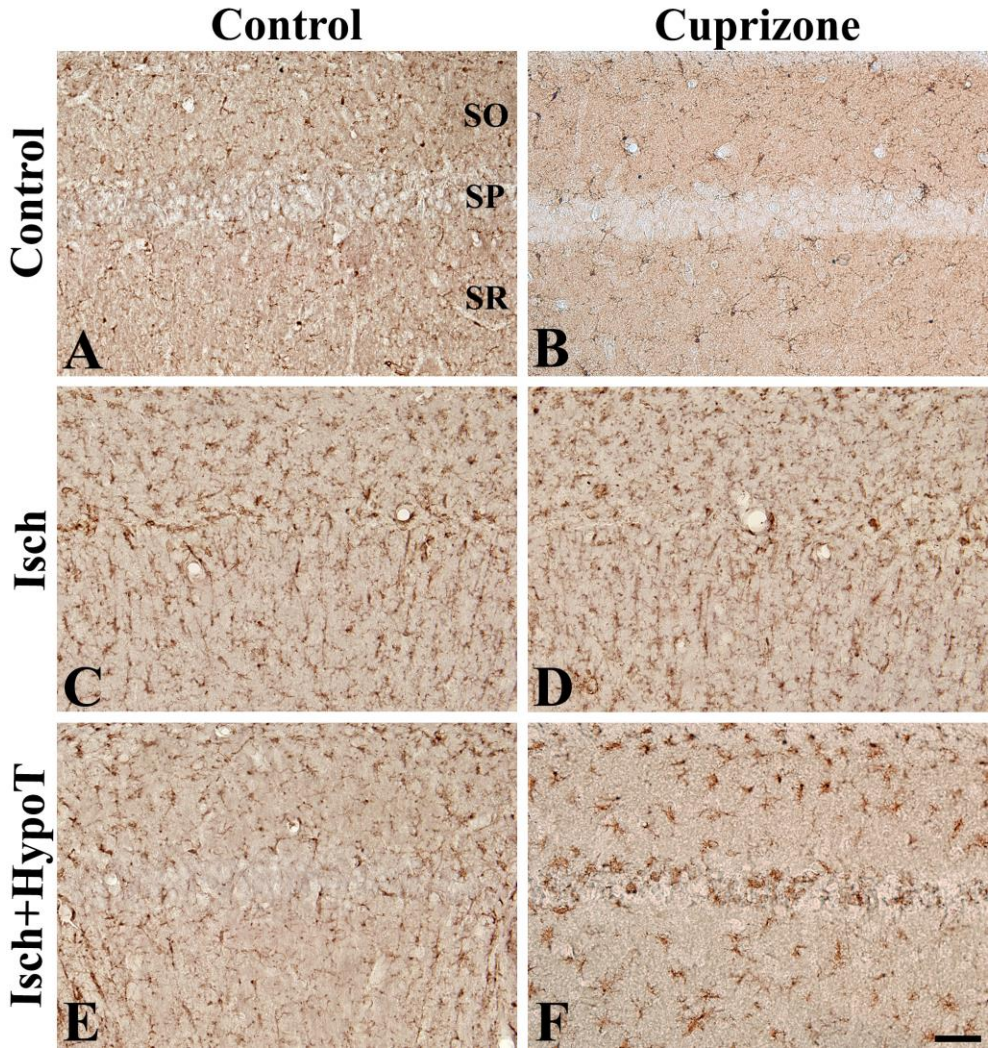
Control
Cuprizone
Control
Isch
Isch+HypoT
SO
SP
SR
A
B
C
D
E
F

Figure 13. Iba-1 immunohistochemistry in the gerbil CA1 region of the hippocampus of the Control (A), Cup (B), Control+Isch (C), Cup+Isch (D), Control+Isch+HypoT (E), and Cup+Isch+HypoT groups (F). SP, stratum pyramidale; SO, stratum oriens; SR, stratum radiatum. Scale bar = 50 μm (n = 5 per group).

Discussion

Experiment 1: Cuprizone and melatonin effect on hippocampal neurogenesis in C57BL/6 mice

Cuprizone effect on hippocampal neurogenesis

Cuprizone, a copper chelator, caused neuronal degeneration including demyelination in various regions of the brain (Stidworthy et al., 2003; Komoly., 2005). In this study, we investigated the effects of cuprizone on hippocampal neurogenesis in healthy mice by immunohistochemistry and protein expression.

Cell proliferation and neuroblast differentiation in the DG of hippocampus were investigated using Ki67 and DCX immunostaining, respectively. Ki67 is expressed in the nucleus during the active cell cycle, except for the resting (G0) and early G1 phases, and therefore, Ki67 is used as a marker for cell proliferation (Cooper-Kuhn and Kuhn., 2002). DCX, which is a microtubule-associated protein, is expressed in neuronal precursor cells, differentiating neuroblasts, and immature neurons, and thus DCX is used as a marker for neuroblast differentiation (Karl et al., 2005). Cuprizone administration significantly decreased the number of Ki67-positive nuclei and immunoreactivity of DCX-positive neuroblasts in the hippocampal DG of mice. These results suggest that cuprizone reduces hippocampal neurogenesis.

Glucose is transported into the brain by a family of facilitative transmembrane transport protein family, GLUTs. Primary isoforms of GLUTs in the brain are GLUT1 and GLUT3. GLUT1 is usually detected in the blood-brain barrier (BBB) and astrocytes; GLUT3 has a major role in glucose uptake in neurons (Rajakumar et al., 1998; Vannucci et al., 1997; Roman et al., 2001). Because GLUT3 facilitates

glucose supply to the neurons even at low interstitial glucose concentration, it is a major glucose transporter within the brain (Roman et al., 2001). In the present study, we found that GLUT3 immunoreactivity was significantly decreased in the SGZ after a 6-week cuprizone diet compared to that after a normal diet. This means that the cuprizone administration affects glucose transport and utilization in the neuron.

Phosphorylation of CREB protein on Ser133 is a rate-limiting pathway in the activity of the CREB-signaling pathway (Gonzalez & Montminy., 1989). In many studies, immunohistochemistry for pCREB was used, and pCREB is present in almost all new-born immature neurons of the SCZ (Merz et al., 2011). Facilitation of pCREB in primary hippocampal neurons was followed by acute and gradual stimulation of BDNF and increased neuronal plasticity (Ji et al., 2010). BDNF, a neurotrophin, promotes newborn neuron survival and maturation (Chan et al., 2008; Choi et al., 2009). In this study, we demonstrated that pCREB- positive nuclei and BDNF expression in the cuprizone group decreased compared to that in the control group. Cuprizone administration impairs hippocampal neurogenesis by decreasing pCREB protein and BDNF expression.

Effects of melatonin on the cuprizone-induced reduction of hippocampal neurogenesis

Cuprizone induces oxidative stress in the CNS, and cuprizone administration for several weeks results in neuronal degeneration such as CNS demyelinatio. In this study, we already demonstrated that cuprizone administration for 6 weeks decreased hippocampal neurogenesis. Melatonin, a neurohormone synthesized in the pineal gland, is a powerful antioxidative and antiexcitotoxic agent, thus acting

as a neuroprotectant against neuronal degeneration (Pandi-Perumal et al., 2013). Recently, in many studies, melatonin focuses on its powerful antioxidant function (Maldonado et al., 2007; Samantaray et al., 2008; Das et al., 2008; Cervantes et al., 2008; Tengattini et al., 2008; Gitto et al., 2009). Melatonin administration affected not only proliferation and differentiation of embryonic neural stem cell (Moriya et al., 2007) but also stimulation of endogenous neurogenesis in the animal model of mild focal ischemia (Kilic et al. 2008). Moreover, melatonin affected hippocampal neurogenesis in the neurodegenerative animal model such as the D-galactose induced aging mouse model (Yoo et al., 2012). Yoo et al. (2012) demonstrated that administration of melatonin ameliorated D-galactose-induced reduction of cell proliferation and neuroblast differentiation in the hippocampal DG.

In this study, the role of melatonin was investigated by immunohistochemistry of Ki67, DCX, GLUT3, and pCREB for cell proliferation, neuroblast differentiation, glucose transport and utilization, and phosphorylation of CREB, respectively. Western blot analysis of BDNF protein was performed for BDNF expression. In the cuprizone + melatonin group, Ki67-positive nuclei and immunoreactivity of DCX-positive neuroblast in the DG of the hippocampus significantly increased compared to those in the cuprizone group. This result is supported by a previous study reporting that melatonin ameliorates reduction in neurogenesis in the D-galactose induced aging animal model (Yoo et al., 2012) or irradiation (Manda et al., 2009).

In the cuprizone + melatonin group, immunoreactivity of GLUT3 in the DG of hippocampus significantly increased compared to that in the cuprizone group. Melatonin administration increased glucose consumption and utilization of the neuron in the SGZ. Glucose is essential for neuronal survival. GLUT for glucose transport and utilization is an essential organelle for neuronal survival. Among the

GLUT, GLUT3 is a major glucose transporter in the brain (Roman et al., 2001). GLUT3 immunoreactivity increases when neurogenesis is high, such as in new-born neuron (Jung et al., 2016) and brain ischemia-induced compensatory neurogenesis (Yoo et al., 2016). Therefore, melatonin administration ameliorated reduction of glucose transport and utilization by cuprizone administration in the neuron.

In the cuprizone + melatonin group, pCREB-positive nuclei and expression of BDNF in the DG of the hippocampus significantly increased compared to that in cuprizone group. Melatonin administration increased phosphorylation of CREB protein and BDNF protein expression. This result is supported by a previous study revealing that administration of melatonin increased immunohistoreactivity of pCREB in D-galactose-induced aging animal models (Yoo et al., 2012). Phosphorylated CREB and BDNF are closely related, and this relationship contributes to neurogenesis (Begni et al., 2017). BDNF, a neurotrophin secreted from the presynaptic neuron, binds to the tropomyosin receptor kinase B (TrkB) in the postsysnaptic membrane. When BDNF binds to TrkB, several downstream signaling pathways, such as the mitogen-activated protein kinase (MAPK), phospholipase C-γ (PLC-γ), and phosphoinositide-3-kinase (PI3K) pathways, are activated (Begni et al., 2017). If the MAPK signaling pathway is activated, extracellular signal-regulated kinase 1/2 (ERK) translocates into the nucleus and, phosphorylates and activates transcription factors such as CREB (Grewal et al., 1999; Shaywitz and Greenberg., 1999). Phosphorylated CREB binds to the BDNF promoter, activates BDNF transcription (Shaywitz and Greenberg., 1999). This BDNF–ERK–CREB signaling plays a major role in neurogenesis by neuronal cell survival, synaptic structure and plasticity (Patapoutian and Reichardt., 2001).

Melatonin administration increased cell signaling related to neurogenesis.

Therefor Melatonin treatment ameliorate cuprizone-induced hippocampal neurogenesis reduction.

Effects of melatonin on the cuprizone-induced changes of pCREB and DCX expression in SCZ

Cuprizone-induced demyelination occurs in the CC (Stidworthy et al., 2003; Komoly et al., 2005). In the normal state, there is no immunoreactivity of pCREB in rats (Kim et al., 2005). Phosphorylation of CREB may be activated form, so it may not be expressed in normal conditions. Cuprizone treatment induced demyelination, and this condition may activate compensatory responses in neurogenesis in the SCZ through the pCREB. A recent study focused on neurogenesis in the SCZ demonstrated that the mature neuron can be generated from neuronal stem cells originating in the SCZ and few neurons from the SCZ can survive and mature under traumatic brain injury (TBI) (Kim et al., 2016). In the present study, pCREB immunoreactivity was not found in the SCZ of the control group. However, in the cuprizone group, pCREB immunoreactivity in the SCZ increased compared to that in the control group. Moreover, melatonin treatment increased pCREB immunoreactivity in the SCZ compared to those in the control and cuprizone groups. However, DCX immunoreactivity slightly increased in the cuprizone group compared to that in the control group, and in the cuprizone + melatonin group it significantly increased compared to those in the control and cuprizone groups. Cuprizone administration increased pCREB significantly and neuroblast differentiation inignificantly in the SCZ. In contrast, melatonin administration significantly increased pCREB and neuroblast differentiation in the

SCZ. Cuprizone and melatonin administration increased neurogenesis in the SCZ. A recent study demonstrated that few neurons originated from the SCZ in TBI and BDNF infusion prevented cell death and atrophy in newborn neurons (Kim et al., 2016). In the present study, cuprizone treatment-induced compensatory neurogenesis initiated in the SCZ, and immunoreactivity of pCREB might be increased. However, cuprizone administration might be insufficient for new-born neurons to survive in the SCZ, so neuroblast differentiation increased compared to the control group, in significantly. However, melatonin administration increased expression of BDNF, a neurotrophic factor; therefore, melatonin administration increased both pCREB and neuroblast differentiation in the SCZ.

Experimental 2: Cuprizone and hypothermia effect on global forebrain ischemia in Mongolian gerbils

Effects of cuprizone on neuronal degeneration induced by ischemic damage

To confirm cuprizone effect on neuronal degeneration in ischemic damage, CV staining and immunohistochemistry of GFAP and Iba-1 in the hippocampal CA1 region were performed. Transient forebrain ischemia in gerbils induces neuronal damage in the CA1 region from the 4th day after ischemic surgery, and this is a specific lesion in the global forebrain ischemia gerbil model. To confirm neuronal death, in this study, CV staining performed in every animal in all groups. Transient forebrain ischemia showed massive neuronal damage in the hippocampal CA1 region of the Control+Isch and Cup+Isch groups, and there were no differences in the number of CV-positive cells between groups.

GFAP is an intermediate filament protein that is expressed by numerous cell including astrocytes in the CNS (Jacque et al., 1978). An astrocyte is a greatly important cell type in the CNS. It plays a role in cell communication and functioning of the BBB. Further, it plays a role in the formation of glial scars in the repair process after CNS injury (Paetau et al., 1985). In this study, GFAP immunoreactivity was evaluated to confirm cuprizone effect on brain ischemic injury. Transient forebrain ischemia showed hypertrophied cytoplasm in the hippocampal CA1 region of the Control+Isch and Cup+Isch groups and there were no remarkable morphological differences in GFAP-positive astrocytes in the CA1 region.

Iba-1 is specifically expressed in cells derived from monocyte lineages. In the CNS, Iba-1 is expressed in microglia, as macrophages in the CNS, and upregulated when

these cells are activated. Microglia are activated when the CNS is injured such as TBI, brain ischemia, and other neurological disorders (Ito et al., 1998). In this study, immunohistochemistry for Iba-1 is performed to confirm the effect of cuprizone on forebrain ischemia. In the Control+Isch group, Iba-1-positive microglia had hypertrophic cytoplasm with thickened processes and there were no remarkable morphological differences in Iba-1-positive astrocytes in the CA1 region between the Control+Isch and Cup+Isch groups.

Effects of cuprizone on ischemia-induced neurogenesis in the DG

When blood supply is interrupted by cardiac arrest or obstruction of blood supply to the brain, it results in neuronal death and eventually loss of function (Bronwen 2012). Recent studies demonstrated that brain ischemic injury dramatically increased neurogenesis in the rodent SGZ of the DG (Lichtenwalner et al., 2006; Liu et al., 1998; Tsai et al., 2011; Arvidsson et al., 2002). In this study, immunohistochemistry of DCX and Ki67 for neuroblast differentiation and cell proliferation, respectively, were performed to confirm cuprizone effect on ischemia-induced hippocampal neurogenesis. Forebrain ischemia increased neuroblast differentiation and cell proliferation in the DG of the hippocampus. However, the Cup+Isch group showed significant decreases in DCX and Ki67 immunoreactivity compared to that in the Control+Isch group. This result suggests that cuprizone administration impairs hippocampal neurogenesis induced by the transient forebrain in the hippocampal CA1 region although they did not show any effects on neuronal damage by transient ischemia.

Effects of cuprizone on hypothermia-induced reduction of cell death on brain ischemia

To confirm the protective effect of hypothermia on brain ischemia in this study, CV staining for cell survival in the CA1 region, immunohistochemistry of DCX and Ki67 for neurogenesis and immunohistochemistry of GFAP and Iba-1 for neuro-inflammation were performed. In the Control+Isch+HypoT group, cell survival in the CA1 region and immunoreactivity for neurogenesis increased compared to that in the Control+Isch group. Similarly, Iba-1 immunoreactivity for neuro-inflammation and reactive astrocytosis decreased compared to those in the Control+Isch group. However, in the Cup+Isch+HypoT group, CV-positive cells were less abundantly found in the CA1 region compared to that in the Control+Isch+HypoT group. Additionally, reactive gliosis by transient forebrain ischemia was more prominent in the CA1 region compared to that in the Control+Isch+HypoT group. Cell proliferation and neuroblast differentiation was also significantly decreased in the Cup+Isch+HypoT group.

In the hypothermic condition, when brain ischemia occurs, brain damage decreases because hypothermia affects the brain damage stage from the acute to chronic phase. In the acute phase, hypothermia affects alteration of cerebral blood flow, preservation of energy stores, reduction of excitatory amino acids, and so on. In the subacute phase, it affects the prevention of apoptotic death, inhibition of inflammation, and reduction of BBB disruption. In the chronic phase of brain damage, hypothermia enhances differentiation of precursor cells and angiogenesis (Yenari et al., 2012). These results suggest that cuprizone-induced demyelination affects neural plasticity induced by hypothermia in the ischemic hippocampus.

Conclusion

In these studies, we investigated the effects of cuprizone on hippocampal plasticity in naïve mice and ischemic gerbils. In C57BL/6 mice, cuprizone treatment decreased Ki67 positive nuclei, immunoreactivity of DCX, and GLUT3, and pCREB positive nuclei. In addition, cuprizone treatment decreased BDNF protein expression. Cuprizone treatment reduced hippocampal neurogenesis and this reduction was ameliorated by melatonin treatment in male C57BL/6 mice.

Transient forebrain ischemia in Mongolian gerbils increased hippocampal neurogenesis in the DG, and neuro-inflammation, and cell apoptosis in the CA1 region of the hippocampus. However, the hypothermia increased hippocampal neurogenesis in the DG and ameliorated brain ischemic damage in the CA1 region of the hippocampus. There were no remarkable differences in brain ischemic damage by cuprizone treatment. However, cuprizone treatment decreased ischemia-induced hippocampal neurogenesis and disturbed the protective effect of hypothermia on brain ischemic damage. Therefore, cuprizone administration reduced hippocampal neurogenesis, which is enhanced by melatonin treatment, and disturbed protective effect of hypothermia in brain ischemia. These results suggest that cuprizone-induced demyelination can be useful model to observe the mechanism of hippocampal neurogenesis.

References

Abdipranoto, A., Wu, S., Stayte, S., Vissel, B., 2008. The role of neurogenesis in neurodegenerative diseases and its implications for therapeutic development. CNS Neurol Disord Drug Targets 7, 187-210.

Arvidsson, A., Collin, T., Kirik, D., Kokaia, Z., Lindvall, O., 2002. Neuronal replacement from endogenous precursors in the adult brain after stroke. Nat Med. 8, 963–970.

Begni, V., Riva, M.A., Cattaneo, A., 2017. Cellular and molecular mechanisms of the brain-derived neurotrophic factor in physiological and pathological conditions. 131, 123-138.

Biebl, M., Cooper, C.M., Winkler, J., Kuhn, H.G., 2000. Analysis of neurogenesis and programmed cell death reveals a selfrenewing capacity in the adult rat brain. Neurosci Lett. 291, 17–20.

Blakemore, W., 1972. Observations on oligodendrocyte degeneration, the resolution of status spongiosus and remyelination in cuprizone intoxication in mice. J Neurocytol. 1, 413-426.

Blakemore, W.F., 1973. Demyelination of the superior cerebellar peduncle in the mouse induced by cuprizone. J Neurol Sci. 20, 63-72.

Bronwen, C: In Compensatory neurogenesis in the injured adult brain, Agrawal, A, eds. Brain Injury – Pathogenesis, Monitoring, Recovery and Management, In Tech, Rijeka, Croatia, 2012, 63-86.

Cervantes, M., Moralı´, G., Letechipı´a-Vallejo, G., 2008. Melatonin and ischemia–reperfusion injury of the brain. J. Pineal Res. 45, 1–7. Moriya, T., Horie, N., Mitome, M., Shinohara, K., 2007. Melatonin influences the proliferative and differentiative activity of neural stem cells. J. Pineal Res. 42, 411–418.

Chan, J.P., Cordeira, J., Calderon, G.A., Iyer, L.K., Rios, M., 2008. Depletion of central BDNF in mice impedes terminal differentiation of new granule neurons in the adult hippocampus. Mol. Cell. Neurosci. 39, 372–383.

Cho, S., Joh, T.H., Baik, H.H., Dibinis, C., Volpe, B.T., 1997. Melatonin administration protects CA1 hippocampal neurons after transient forebrain ischemia in rats. Brain Res. 755, 335–338.

Choi, S.H., Li, Y., Parada, L.F., Sisodia, S.S., 2009. Regulation of hippocampal progenitor cell survival, proliferation and dendritic development by BDNF. Mol Neurodegener. 4, 52.

Chugani, H.T., 1998. A critical period of brain development: studies of cerebral glucose utilization with PET. Prev Med 27, 184-188.

Compston, A,, Coles, A., 2008. Multiple sclerosis. Lancet. 372, 1502–1517.

Cooper-Kuhn, C.M., Kuhn, H.G., 2002. Is it all DNA repair?: methodological considerations for detecting neurogenesis in the adult brain. Brain Res Dev Brain Res. 134, 13-21.

Das, A., Belagodu, A., Reiter, R.J., Ray, S.K., Banik, N.L., 2008. Cytoprotective effects of melatonin on C6 astroglial cells exposed to glutamate excitotoxicity and oxidative stress. J. Pineal Res. 45, 117–124.

Das, A., McDowell, M., Pava, M.J., Smith, J.A., Reiter, R.J., Woodward, J.J., Varma, A.K., Ray, S.K., Banik, N.L., 2010. The inhibition of apoptosis by melatonin in VSC4.1 motoneurons exposed to oxidative stress, glutamate excitotoxicity, or TNF-a toxicity involves membrane melatonin receptors. J Pineal Res. 48, 157–169.

Encinas, J.M., Vaahtokari, A., Enikolopov, G., 2006. Fluoxetine targets early progenitor cells in the adult brain. Proc Natl Acad Sci. 103, 8233–8238.

Galano, A., Tan, D.X., Reiter, R.J., 2011. Melatonin as a natural ally against oxidative stress: a physicochemical examination. J Pineal Res. 51, 1–16.

Ge, S., Pradhan, D.A., Ming, G.L., Song, H., 2007. GABA sets the tempo for activity-dependent adult neurogenesis. Trends Neurosci. 30, 1–8.

Gitto, E., Pellegrino, S., Gitto, P., Barberi, I., Reiter, R.J., 2009. Oxidative stress of the newborn in the pre- and postnatal period and the clinical utility of melatonin. J. Pineal Res. 46, 128–139.

Giusti, P., Lipartiti, M., Franceschini, D., Schiavo, N., Floreani, M., Manev, H., 1996. Neuroprotection by melatonin from kainate-induced excitotoxicity in rats. FASEB J. 10, 891–896.

Gonzalez, G.A., Montminy, M.R., 1989. Cyclic AMP stimulates somatostatin gene transcription by phosphorylation of CREB at serine 133. Cell, 59, 675–680.

Goodman, T., Trouche, S., Massou, I., Verret, L., Zerwas, M., Roullet, P., Rampon, C., 2010. Young hippocampal neurons are critical for recent and remote spatial memory in adult mice. Neuroscience. 171, 769-778.

Green, D.R., Reed, J.C., 1998. Mitochondria and apoptosis. Science. 281, 1309–1312.

Grewal, S.S., York, R.D., Stork, P.J., 1999. Extracellular-signal-regulated kinase signalling in neurons. Curr. Opin. Neurobiol. 9, 544–553.

Gross, A., McDonnell, J.M., Korsmeyer, S.J., 1999. BCL-2 family members and the mitochondria in apoptosis. Genes Dev. 13, 1899–1911.

Gudi, V., Gingele, S., Skripuletz, T., Stangel, M., 2014. Glial response during cuprizone-induced de- and remyelination in the CNS: lessons learned. Front Cell Neurosci. 8: 73.

Harput, U.S., Genc, Y., Saracoglu, I., 2012. Cytotoxic and antioxidative activities of Plantago lagopus L. and characterization of its bioactive compounds. Food Chem. Toxicol. 50, 1554–1559.

Hardeland, R., Pandi-Perumal, S.R., Cardinali, D.P., 2006. Melatonin. Int J Biochem Cell Biol. 38, 313–316.

Hillis, J.M., Davies, J., Mundim, M.V., Al-Dalahmah, O., Szele, F.G., 2016 Cuprizone demyelination induces a unique inflammatory response in the subventricular zone. J Neuroinflammation. 13, 190-205.

Hwang, I.K., Eum, W.S., Yoo, K.Y., Cho, J.H., Kim, D.W., Choi, S.H., Kang, T.C., Kwon, O.S., Kang, J.H., Choi, S.Y., Won, M.H., 2005. Copper chaperone for Cu, Zn-SOD supplement potentiates the Cu, Zn-SOD function of neuroprotective effects against ischemic neuronal damage in the gerbil hippocampus. Free Radic Biol Med. 39, 392–402.

Hwang, I.K., Yoo, K.Y., Kim, D.W., Lee, C.H., Choi, J.H., Kwon, Y.G., Kim, Y.M., Choi, S.Y., Won, M.H., 2010. Changes in the expression of mitochondrial peroxiredoxin and thioredoxin in neurons and glia and their protective effects in experimental cerebral ischemic damage. Free Radic Biol Med. 48, 1242–1251.

Ito, D., Imai, Y., Ohsawa, K., Nakajima, K., Fukuuchi, Y., Kohsaka, S., 1998. Microglia-specific localisation of a novel calcium binding protein, Iba1. Brain Res Mol Brain Res. 57, 1–9.

Jacque, C.M., Vinner, C., Kujas, M., Raoul, M., Racadot, J., Baumann, N.A., 1978. Determination of glial fibrillary acidic protein (GFAP) in human brain tumors. J Neurol Sci. 35, 147–155.

Ji, Y., Lu, Y., Yang, F., Shen, W., Tang, T.T., Feng, L., Duan, S., Lu, B., 2010 Acute and gradual increases in BDNF concentration elicit distinct signaling and functions in neurons. Nat. Neurosci. 13, 302–309.

Jou, M.J., Peng, T.I., Hsu, L.F., Jou, S.B., Reiter, R.J., Yang, C.M., Chiao, C.C., Lin, Y.F., Chen, C.C., 2010. Visualization of melatonin's multiple mitochondrial levels of protection against mitochondrial Ca(2+)-mediated permeability transition and beyond in rat brain astrocytes. J Pineal Res. 48, 20–38.

Jung, H.Y., Yim, H.S., Yoo, D.Y., Kim, J.W., Chung, J.Y., Seong, J.K., Yoon, Y.S., Kim, D.W., Hwang, I.K., 2016. Postnatal changes in glucose transporter 3 expression in the dentate gyrus of the C57BL/6 mouse model. Lab Anim Res. 32, 1-7.

Karl, C., Couillard-Despres, S., Prang, P., Munding, M., Kilb, W., Brigadski, T., Plötz, S., Mages, W., Luhmann, H., Winkler, J., Bogdahn, U., Aigner, L., 2005. Neuronal precursor-specific activity of a human doublecortin regulatory sequence. J Neurochem. 92, 264-282.

Kempermann G1, Song H2, Gage FH3., 2015. Neurogenesis in the Adult Hippocampus. Cold Spring Harb Perspect Biol. 1, 7-22.

Kesterson, J.W., Carlton, W.W. 1971. Histopatholoic and enzyme histochemical observations of the cuprizoneinduced brain edema. Exper Mol Pathol. 15,82-96.

Kilic, E., Ozdemir, Y.G., Bolay, H., Keleştimur, H., Dalkara, T., 1999. Pinealectomy aggravates and melatonin administration attenuates brain damage in focal ischemia. J Cereb Blood Flow Metab. 19, 511–516.

Kim, D.W., Chang, J.H., Park, S.W., Jeon, G.S., Seo, J.H., Cho, S.S., 2005. Activated cyclic AMP-response element binding protein (CREB) is expressed in a myelin-associated protein in chick. Neurochem Res. 30, 1133-1137.

Kim, J.Y., Choi, K., Shaker, M.R., Lee, J.H., Lee, B., Lee, E., Park, J.Y., Lim, M.S., Park, C.H., Shin, K.S., Kim, H., Geum, D., Sun, W., 2016. Promotion of cortical neurogenesis from the neural stem cells in the adult mouse subcallosal zone. Stem Cells. 34, 888-901.

Kirino, T., 1982. Delayed neuronal death in the gerbil hippocampus following ischemia. Brain Res. 239, 57–69.

Komoly, S., 2005. Experimental demyelination caused by primary oligodendrocyte dystrophy. Regional distribution of the lesions in the nervous system of mice. Ideggyogy Sz. 58, 40-43.

Kronenberg, G., Reuter, K., Steiner, B., Brandt, M.D., Jessberger, S., Yamaguchi, M., Kempermann, G., 2003. Subpopulations of proliferating cells of the adult hippocampus respond differently to physiologic neurogenic stimuli. J CompNeurol. 467, 455–463.

Kuhn, H.G., Biebl, M., Wilhelm, D., Li, M., Friedlander, R.M., Winkler, J., 2005. Increased generation of granule cells in adult Bcl-2-overexpressing mice: A role for cell death during continued hippocampal neurogenesis. Eur J Neurosci. 22, 1907–1915.

Loskota, W.A, Lomax, P., Verity, M.A., A Stereotaxic Atlas of the Mongolian Gerbil Brain (Meriones unguiculatus). Ann Arbor Science Publishers Inc., Ann Arbor, 1974.

Lichtenwalner, R.J., Parent, J.M., 2006. Adult neurogenesis and the ischemic forebrain. J Cereb Blood Flow Metab. 26, 1–20.

Lin, C.S., Polsky, K., Nadler, J.V., Crain, B.J., 1990. Selective neocortical and thalamic cell death in the gerbil after transient ischemia. Neuroscience. 35, 289–299.

Liu, J., Solway, K., Messing, R.O., Sharp, F.R., 1998. Increased neurogenesis in the dentate gyrus after transient global ischemia in gerbils. J Neurosci. 18, 7768–7778.

Ludwin, S., 1994. Central nervous system remyelination: studies in chronically damaged tissue. Ann Neurol. 36, Suppl:143-145.

Maldonado, M.D., Murillo-Cabezas, F., Terron, M.P., Flores, L.J., Tan, D.X., Manchester, L.C., Reiter, R.J., 2007. The potential of melatonin in reducing morbiditymortality after craniocerebral trauma. J. Pineal Res. 42, 1–11.

Manda, K., Ueno, M., Anzai, K., 2008. Space radiation-induced inhibition of neurogenesis in the hippocampal dentate gyrus and memory impairment in mice: ameliorative potential of the melatonin metabolite, AFMK. J Pineal Res. 45, 430–438.

Manev, H., Uz, T., Kharlamov, A., Joo, J.Y., 1996. Increased brain damage after stroke or excitotoxic seizures in melatonin-deficient rats. FASEB J. 10, 1546–1551.

Manda, K., Ueno, M., Anzai, K., 2009. Cranial irradiation-induced inhibition of neurogenesis in hippocampal dentate gyrus of adult mice: attenuation by melatonin pretreatment. J Pineal Res. 46, 71–78.

Merz, K., Herold, S., Lie, D.C., 2011. CREB in adult neurogenesis--master and partner in the development of adult-born neurons? Eur J Neurosci. 33, 1078-1086.

Miyata, T., Ono, Y., Okamoto, M., Masaoka, M., Sakakibara, A., Kawaguchi, A., Hashimoto, M., Ogawa, M., 2010. Migration, early axonogenesis, and Reelin-dependent layer-forming behavior of early/posterior-born Purkinje cells in the developing mouse lateral cerebellum. Neural Dev. 5, 1-21.

Moskowitz, M.A., Lo, E.H., Iadecola, C., 2010. The science of stroke: mechanisms in search of treatments. Neuron. 67, 181–198.

Moriya, T., Horie, N., Mitome M., Shinohara, K., 2007. Melatonin influences the proliferative and differentiative activity of neural stem cells. J Pineal Res. 42, 411–418.

Paetau, A., Elovaara, I., Paasivuo, R., Virtanen, I., Palo, J., Haltia, M., 1985. Glial filaments are a major brain fraction in infantile neuronal ceroid-lipofuscinosis. Acta Neuropathol. 65, 190–194.

Pandi-Perumal, S.R., BaHammam, A.S., Brown, G.M., Spence, D.W., Bharti, V.K., Kaur, C., Hardeland, R., Cardinali, D.P., 2013. Melatonin antioxidative defense: therapeutical implications for aging and neurodegenerative processes. Neurotox Res. 23, 267-300.

Paradies, G., Petrosillo, G., Paradies, V., Reiter, R.J., Ruggiero, F.M., 2010. Melatonin, cardiolipin and mitochondrial bioenergetics in health and disease. J Pineal Res. 48, 297–310.

Patapoutian, A., Reichardt, L.F., 2001. Trk receptors: mediators of neurotrophin action. Curr. Opin. Neurobiol. 11, 272–280.

Pattison, I.H., Jebbett, J.N., 1971. Clinical and histological observations on cuprizone toxicity and scrapie in mice. Res Vet Sci. 12, 378-380.

Paxinos G and Franklin KBJ: The mouse brain in stereotaxic coordinates. Academic Press, San Diego, 2001.

Petito, C.K., Torres-Munoz, J., Roberts, B., Olarte, J.P., Nowak Jr. T.S., Pulsinelli, W.A., 1997. DNA fragmentation follows delayed neuronal death in CA1 neurons exposed to transient global ischemia in the rat. J. Cereb. Blood Flow Metab. 17, 967–976.

Praet, J., Guglielmetti, C., Berneman, Z., Van der Linden, A., Ponsaerts, P., 2014. Cellular and molecular neuropathology of the cuprizone mouse model: clinical relevance for multiple sclerosis. Neurosci Biobehav Rev. 47, 485-505.

Rajakumar, R.A., Thamotharan, S., Menon, R.K., Devaskar, S.U., 1998. Sp1 and Sp3 regulate transcriptional activity of the facilitative glucose transporter isoform-3 gene in mammalian neuroblasts and trophoblasts. J Biol Chem. 273, 27474-27483.

Ramírez-Rodríguez, G., Klempin, F., Babu, H., Benítez-King, G., Kempermann, G., 2009. Melatonin modulates cell survival of new neurons in the hippocampus of adult mice. Neuropsychopharmacology. 34, 2180–2191.

Ramirez-Rodriguez, G., Ortíz-López, L., Domínguez-Alonso, A., Benítez-King, G.A., Kempermann, G., 2011. Chronic treatment with melatonin stimulates dendrite maturation and complexity in adult hippocampal neurogenesis of mice. J Pineal Res. 50, 29–37.

Reiter, R.J., 1998. Oxidative damage in the central nervous system: protection by melatonin. Prog Neurobiol. 56, 359–384.

Reiter, R.J., Manchester, L.C., Tan, D.X., 2010. Neurotoxins: free radical mechanisms and melatonin protection. Curr Neuropharmacol. 8, 194–210.

Rennie, K., De Butte, M., Pappas, B.A., 2009. Melatonin promotes neurogenesis in dentate gyrus in the pinealectomized rat. J Pineal Res. 47, 313–317.

Rodriguez, C., Mayo, J.C., Sainz, R.M., Antolín, I., Herrera, F., Martín, V., Reiter, R.J., 2004. Regulation of antioxidant enzymes: a significant role for melatonin. J Pineal Res. 2004; 36, 1–9.

Samantaray, S., Sribnick, E.A., Das, A., Knaryan, V.H., Matzelle, D.D., Yallapragada, A.V., Reiter, R.J., Ray, S.K., Banik, N.L., 2008. Melatonin attenuates calpain upregulation, axonal damage and neuronal death in spinal cord injury in rats. J. Pineal Res. 44, 348–357.

Shaywitz, A.J. and Greenberg, M.E., 1999. CREB: a stimulus-induced transcription factor activated by a diverse array of extracellular signals. Annu. Rev. Biochem. 68, 821–861.

Shaywitz, A.J. and Greenberg, M.E. (1999) CREB: a stimulus-induced transcription factor activated by a diverse
array of extracellular signals. Annu. Rev. Biochem. 68,
821–861

Soler, E.P., Ruiz, V.C., 2010. Epidemiology and risk factors of cerebral ischemia and ischemic heart diseases: similarities and differences. Curr Cardiol Rev. 6, 138-149.

Sotthibundhu, A., Phansuwan-Pujito, P., Govitrapong, P., 2010. Melatonin increases proliferation of cultured neural stem cells obtained from adult mouse subventricular zone. J Pineal Res. 49, 291–300.

Stidworthy, M.F., Genoud, S., Suter, U., Mantei, N., Franklin, R.J., 2003. Quantifying the early stages of remyelination following cuprizone-induced demyelination. Brain Pathol. 13, 329-39.

Suzuki, K., Kikkawa, T., 1969. Status spongiosus of CNS and hepatic changes induced by curpizone (biscyclohexanone oxalyldihydrazone). Am J Pathol. 54, 307-325.

Tan, D.X., Chen, L.D., Poeggeler, B., Manchester, L.C., Reiter, R.J., 1993. Melatonin: a potent endogenous hydroxyl radical scavenger. Endocr J. 1, 57–60.

Tengattini, S., Reiter, R.J., Tan, D.X., Terron, M.P., Rodella, L.F., Rezzani, R., 2008. Cardiovascular diseases: protective effects ofmelatonin. J. Pineal Res. 44, 16–25.

Thamotharan, S., Stout, D., Shin, B.C., Devaskar, S.U., 2013. Temporal and spatial distribution of murine placental and brain GLUT3-luciferase transgene as a readout of in vivo transcription. Am J Physiol Endocrinol Metab. 304, E254-E266.

Toni, N., Schinder, A.F., 2015. Maturation and Functional Integration of New Granule Cells into the Adult Hippocampus. Cold Spring Harb Perspect Biol. 8, a018903

Tozuka, Y., Fukuda, S., Namba, T., Seki, T., Hisatsune, T., 2005. GABAergic excitation promotes neuronal differentiation in adult hippocampal progenitor cells. Neuron. 47, 803–815.

Tsai, Y.W., Yang, Y.R., Wang, P.S., Wang, R.Y., 2011 Intermittent hypoxia after transient focal ischemia induces hippocampal neurogenesis and c-Fos expression and reverses spatial memory deficits in rats. PloS One, 6, e24001.

Vannucci, S.J., Maher, F., Simpson, I.A., 1997. Glucose transporter proteins in brain: delivery of glucose to neurons and glia. Glia. 21, 2-21.

Venturini, G., 1973. Enzymic activities and sodium, potassium and copper concentrations in mouse brain and liver after cuprizone treatment in vivo. J Neurochem. 21, 1147-1151.

Wang, L.P., Kempermann, G., Kettenmann, H., 2005. A subpopulation of precursor cells in the mouse dentate gyrus receives synaptic GABAergic input. Mol Cell Neurosci. 29, 181–189.

Wang, J., Yu, S., Jiao, S., Lv, X., Ma, M., Du, Y., 2013. Kappa-Selenocarrageenan prevents microcystin-LR-induced hepatotoxicity in BALB/c mice. Food Chem. oxicol. 59, 303–310.

Xing, Y.L., Röth, P.T., Stratton, J.A., Chuang, B.H., Danne, J., Ellis, S.L., Ng, S.W., Kilpatrick, T.J., Merson, T.D., 2014. Adult neural precursor cells from the subventricular zone contribute significantly to oligodendrocyte regeneration and remyelination. J Neurosci. 34, 14128–14146.

Yenari, M.A., Han, H.S., 2012. Neuroprotective mechanisms of hypothermia in brain ischaemia. Nat Rev Neurosci. 13, 267-278.

Yoo, D.Y., Kim, W., Lee, C.H., Shin, B.N., Nam, S,M., Choi, J.H., Won, M.H., Yoon, Y.S., Hwang, I.K., 2012. Melatonin improves D-galactose-induced aging effects on behavior, neurogenesis, and lipid peroxidation in the mouse dentate gyrus via increasing pCREB expression. J Pineal Res. 52, 21-28.

Yoo, D.Y., Lee, K.Y., Park, J.H., Jung, H.Y., Kim, J.W., Yoon, Y.S., Won, M.H., Choi, J.H., Hwang, I.K., 2016 Glucose metabolism and neurogenesis in the gerbil hippocampus after transient forebrain ischemia. Neural Regen Res. 11, 1254-1259.

국문초록

Cuprizone은 구리 킬레이터로서 세포의 신진대사를 흔들고 탈수초현상을 일으켜 계속 투여할 경우 별아교세포와 신경세포의 세포사 등을 유발하여 결국 퇴행성 신경 변화를 유발한다. Cuprizone은 음식물에 첨가하여 투여하면 되는 실험적 편의성과 그 가역성 덕분에 실험적으로 많이 사용되고 있다.

이번 실험의 목적은 마우스 정상 동물모델과 저빌을 이용한 앞뇌허혈 동물모델에서 cuprizone이 해마에서의 신경세포재생에 미치는 영향을 알아보고, 특히 이러한 모델 동물에서 멜라토닌과 저체온증의 역할을 확인하기 위한 것이다. 마우스 실험을 위해 8주령의 C57BL/6J 마우스를 무작위로 대조군, cuprizone 투여군, cuprizone과 멜라토닌을 같이 투여한 군으로 나누었다. Cuprizone은 사료에 0.2%의 농도로 함유하도록 제작하여 자유롭게 먹을 수 있도록 하였으며, 멜라토닌은 음수에 6 g/L의 농도로 희석하여 자유롭게 마실 수 있도록 공급하였다. 물질 투여 6주 후에 동물을 희생하여 면역조직화학적염색 및 단백질 정량을 통해서 cuprizone 및 멜라토닌이 신경세포재생에 미치는 영향을 확인하였다. Cuprizone이 저빌의 앞뇌허혈 동물모델에 미치는 영향을 확인하기 위하여, 6주령 저빌을 대상으로 다음과 같은 투여 및 수술을 진행하였다. 앞뇌허혈 수술을 하지 않고 일반 사료를 먹인 군, 앞뇌허혈 수술을 하지 않고 cuprizone을 함유한 사료를 먹인 군, 6주간 일반 사료를 먹인 뒤 정상체온을 유지하며 앞뇌허혈을 유도한 군, 6주간 일반 사료를 먹인 뒤 저체온을 유지하며 앞뇌허혈을 유도한 군, 6주간 cuprizone을 함유한 사료를 먹인 뒤 정상체온을 유지하며 앞뇌허혈을 유도한 군, 6주간 cuprizone을 함유한 사료를 먹인 뒤 저체온을 유지하며 앞뇌허혈을

유도한 군 등 6개의 군으로 나누었다. 앞의 마우스 실험과 마찬가지로 cuprizone은 사료에 0.2%의 농도로 cuprizone을 함유하도록 만들어 자유롭게 먹을 수 있도록 하였다. 앞뇌허혈 수술은 동맥류클립을 이용하여 5분간 온목동맥을 결찰한 다음, 풀어 주어 혈류량이 돌아오는 것을 확인하는 방식으로 진행하였다. 수술 후 2주 뒤에 동물을 희생하여 면역조직화학염색방법을 통해 cuprizone 및 저체온증이 뇌허혈에 미치는 영향을 확인하였다.

마우스 실험에서 cuprizone의 투여는 신경모세포의 분화 및 세포증식을 유의적으로 감소시켰다. 또한 신경세포의 포도당 이용 및 신경세포 내 활성 조절 인자의 전사를 감소시켰다. 그러나, 멜라토닌의 투여는 cuprizone에 의해 감소된 신경모세포의 분화, 세포증식, 신경세포의 포도당 이용 및 신경세포 내 활성 조절 인자의 전사를 증가시켰다. 저빌의 뇌허혈 실험에서 앞뇌허혈에 의해 해마의 CA1영역에서 광범위한 신경세포손상이 유발되었으며, 신경세포재생과 미세아교세포 및 별아교세포의 면역원성이 증가하였다. 그러나 뇌허혈 시 저체온을 유지할 경우 세포의 손상이 억제되었으며, 신경세포재생이 증가하였고 미세아교세포 및 별아교세포의 면역원성이 감소함을 확인하였다. 이러한 저체온에 의한 뇌허혈에서의 변화가 cuprizone투여에 의하여 해마의 CA1영역에서 세포의 생존이 감소하였고, 뇌허혈에 의해서 보상적으로 나타나는 신경세포재생이 감소하였으며, 미세아교세포 및 별아교세포의 면역원성은 증가하였다. 이는 저체온에 의한 뇌허혈의 보호효과가 cuprizone의 투여에 의하여 방해 받는다는 것을 말해준다.

위 실험을 통하여 마우스 정상 동물모델 및 저빌을 이용한 앞뇌허혈 동물모델에서의 cuprizone이 해마에서의 신경세포재생에 미치는 효과와 이에 대한 멜라토닌 및 저체온증의 역할을 면역조직화학염색 및 단백질

분석 등의 실험적 방법을 통해 확인하였다. 본 연구를 통해서 cuprizone의 투여가 해마의 신경세포재생을 저해하고 이것이 멜라토닌에 의해 향상될 수 있음을 확인하였다. 또한 cuprizone의 투여가 뇌에서 허혈성 손상에 따른 세포가소성을 억제하고, 저체온에 의한 허혈성 손상의 보호효과를 방해한다는 것을 확인하였다. 따라서 본 연구는 cuprizone의 투여에 의한 신경손상 동물모델은 해마에서 신경세포재생의 기작을 밝히는데 유용한 모델이 될 수 있음을 시사한다.

주요어 : 큐프리존, 해마, 신경세포재생, 전뇌허혈, 저체온, 멜라토닌, C57BL/6 마우스, 몽고 저빌
학번 : 2011-21683